

2D CFT and efficient Bethe ansatz for exactly solvable Richardson–Gaudin models

Grzegorz Biskowski, Franco Ferrari, Marcin R. Piątek

Institute of Physics, University of Szczecin, Wielkopolska 15, 70–451 Szczecin, Poland
E-mail: biskowski.grzegorz@gmail.com, franco.ferrari@usz.edu.pl,
marcin.piątek@usz.edu.pl

ABSTRACT: This work inaugurates a series of complementary studies on Richardson–Gaudin integrable models. We begin by reviewing the foundations of classical and quantum integrability, recalling the algebraic Bethe ansatz solution of the Richardson (reduced BCS) and Gaudin (central spin) models, and presenting a proof of their integrability based on the Knizhnik–Zamolodchikov equations and their generalizations to perturbed affine conformal blocks. Building on this foundation, we then describe an alternative CFT-based formulation. In this approach, the Bethe ansatz equations for these exactly solvable models are embedded within two-dimensional Virasoro CFT via irregular, degenerate conformal blocks. To probe new formulations within the Richardson–Gaudin class, we develop a high-performance numerical solver. The Bethe roots are encoded in the Baxter polynomial, with initial estimates obtained from a secular matrix eigenproblem and subsequently refined using a deflation-assisted hybrid Newton–Raphson/Laguerre algorithm. The solver proves effective in practical applications: when applied to picket-fence, harmonic oscillator, and hydrogen-like spectra, it accurately reproduces known rapidity trajectories and reveals consistent merging and branching patterns of arcs in the complex rapidity plane. We also explain how to generalize our computational approach to finite temperatures, allowing us to calculate temperature-dependent pairing energies and other thermodynamic observables directly within the discrete Richardson model. We propose an application of the solver to Gaudin-type Bethe equations, which emerge in the classical (large central charge) limit of Virasoro conformal blocks. We conclude by outlining future directions: direct minimization of the Yang–Yang function as an alternative root-finding strategy; revisiting time-dependent extensions; and exploration of complementary analytic frameworks, including matrix models, 2D CFT techniques, and 4D gauge theory/2D CFT dualities.

KEYWORDS: Conformal and W Symmetry, Bethe Ansatz

Contents

1	Introduction	2
2	Integrability and the algebraic Bethe ansatz	3
2.1	Classical integrability	3
2.2	Quantum integrability	9
2.3	Algebraic Bethe ansatz	10
3	Richardson–Gaudin models and Bethe equations	11
3.1	The Richardson model	11
3.2	Gaudin spin models and the conserved charges of the Richardson model	14
3.3	Realization via 2D conformal field theory	17
4	Eigenvalue–based reformulation	20
4.1	Eigenvalue–based method	20
4.2	Application to Richardson’s equations	23
5	Numerical implementation	24
5.1	LU decomposition	25
5.2	Newton–Raphson method	26
5.3	Laguerre method for root finding	26
5.4	Code structure	27
6	Example calculations and applications	29
6.1	Non–degenerate solutions	29
6.2	Degenerate solutions	31
6.3	Thermal pairing	33
6.4	Yang–Yang function and classical conformal blocks	34
7	Conclusions and outlook	37
A	Derivation of the Poisson bracket of Lax matrices	39
B	Hard–core boson algebra	40
C	Derivation of the Richardson equations	42
D	Rank–one irregular state and irregular vertex operator	47

1 Introduction

Quantum integrable models occupy a central place in the study of strongly correlated many-body systems, offering exact analytical control over non-perturbative phenomena ranging from superconductivity to nuclear pairing and quantum magnetism. Among these, the Richardson–Gaudin (RG) family of models [1, 2] provides a paradigmatic example: the exactly solvable pairing Hamiltonian introduced by Richardson and Sherman [3, 4] describes fermions interacting through an attractive pairing force, while the Gaudin spin magnets [5, 6] capture the dynamics of spins coupled via long-range exchange. These models admit Bethe ansatz solutions, in which the many-body spectrum is encoded in a set of nonlinearly coupled algebraic equations for rapidities (Bethe roots).

The primary objective of this paper is to review the standard Bethe ansatz formulation of Richardson–Gaudin models and to reexamine their established connection with two-dimensional conformal field theory (2D CFT) as described in the seminal work [7]. Building on this foundation, we present a CFT-based realization of the Yang–Yang (YY) function that offers an alternative to the construction proposed in [7] by employing irregular, degenerate Virasoro conformal blocks.¹ This representation offers new analytic tools for studying the spectra of RG models.²

Beyond their intrinsic mathematical elegance, RG models find wide application across condensed matter and nuclear physics. The reduced BCS Hamiltonian lies at the heart of superconductivity in metallic grains and governs the crossover from few-to many-particle pair excitations in ultracold atomic gases confined to small reservoirs [8–10]—situations in which discrete energy levels demand an exact treatment. Gaudin magnets, in turn, provide insight into spin wave dynamics in quantum dots and central spin decoherence in spin-qubit devices [11]. In all cases, extracting physical observables such as ground state energy, excitation spectra, and correlation functions relies on the numerical solution of Richardson (Bethe) equations as a function of the coupling constant g .

The second objective of this work is to develop robust numerical methods for tracking rapidities as the coupling g varies, with direct applications to the Richardson equations. This paper also serves as a report on the implementation and testing of these methods and includes a link to the publicly available code (see subsection 5.4), which we release for community use. Our numerical procedure comprises two steps: (i) an eigenvalue-based method that reformulates the Bethe equations as the logarithmic derivative of the Baxter polynomial [12]; and (ii) determining the coefficients of the Baxter polynomial using the Newton–Raphson method combined with LU decomposition, followed by direct root finding via the Laguerre method, enhanced through systematic polynomial deflation.

¹Recall that the YY function serves as the generating potential for the Bethe equations.

²To our knowledge, this observation has not been explicitly addressed in the context of Richardson–Gaudin models.

Our goal was to develop a flexible code that can be easily adapted to different tasks. For example, it reproduces known numerical dependencies of the rapidities on g in both non-degenerate and degenerate regimes. It also supports testing new hypotheses—such as the correspondence between RG models and 2D CFT or other novel formulations described in the conclusions.

The paper is organized as follows. In section 2, with an emphasis on self-contained exposition, we review the foundations of classical and quantum integrability and introduce the algebraic Bethe ansatz. This section draws on the comprehensive review [13] and references therein. In section 3, we present the Richardson–Gaudin models: we derive the Richardson equations, discuss the connection between the reduced BCS model and Gaudin spin systems (informed by [1, 2, 7, 8, 14, 15]), and describe the embedding of these models within 2D CFT [7]. We also introduce our key observation: an alternative representation of the Yang–Yang function using irregular Virasoro blocks. In section 4, we review the eigenvalue-based method for solving the Richardson equations via their correspondence to ordinary differential equations, following [12]. Section 5 details our numerical implementation—based on techniques from [16]—and describes the code architecture. Section 6 presents our numerical results, including graphical visualizations of ground-state rapidities as functions of the coupling g across various models and parameter regimes. We then propose an extension of our computational framework to finite temperatures, enabling direct computation of temperature-dependent pairing energies and other thermodynamic observables in the discrete Richardson model, and outline how the solver can be applied to Gaudin-type Bethe equations arising in the classical limit of Virasoro conformal blocks. Finally, section 7 summarizes our main findings and outlines prospects for future research.

2 Integrability and the algebraic Bethe ansatz

2.1 Classical integrability

Let us consider a $2n$ -dimensional phase space with canonical coordinates $\{q_i\}$ and conjugate momenta $\{p_i\}$, for $i = 1, \dots, n$. For two sufficiently smooth functions $F(q_i, p_i)$ and $G(q_i, p_i)$ defined on this phase space, the *Poisson bracket* $\{F, G\}$ is defined as

$$\{F, G\} \equiv \sum_{i=1}^n \left(\frac{\partial F}{\partial q_i} \frac{\partial G}{\partial p_i} - \frac{\partial F}{\partial p_i} \frac{\partial G}{\partial q_i} \right). \quad (2.1)$$

The Poisson bracket satisfies several important properties: it is bilinear, antisymmetric,

$$\{F, G\} = -\{G, F\},$$

and obeys the Jacobi identity,

$$\{F, \{G, H\}\} + \{G, \{H, F\}\} + \{H, \{F, G\}\} = 0,$$

for any smooth functions F, G, H . These properties make the Poisson bracket a fundamental structure in the study of classical integrable systems.

Let us consider a smooth function $F(\{q_i\}, \{p_i\})$ defined on a $2n$ -dimensional phase space. Its time derivative is given by

$$\dot{F} \equiv \frac{dF}{dt} = \frac{d}{dt} \left[\sum_{i=1}^n \left(\frac{\partial F}{\partial q_i} dq_i + \frac{\partial F}{\partial p_i} dp_i \right) \right] = \sum_{i=1}^n \left(\frac{\partial F}{\partial q_i} \frac{dq_i}{dt} + \frac{\partial F}{\partial p_i} \frac{dp_i}{dt} \right). \quad (2.2)$$

According to Hamilton's canonical equations, we have

$$\frac{dq_i}{dt} = \frac{\partial H}{\partial p_i}, \quad \frac{dp_i}{dt} = -\frac{\partial H}{\partial q_i}. \quad (2.3)$$

Substituting these into equation (2.2), we obtain

$$\dot{F} = \sum_{i=1}^n \left(\frac{\partial F}{\partial q_i} \frac{\partial H}{\partial p_i} - \frac{\partial F}{\partial p_i} \frac{\partial H}{\partial q_i} \right) = \{F, H\}, \quad (2.4)$$

where $\{F, H\}$ denotes the Poisson bracket of F and H .

If the Poisson bracket of two functions vanishes, i.e., $\{F, G\} = 0$, we say that the functions F and G are *in involution*. From equation (2.4), it follows that if a function F is in involution with the Hamiltonian H , then its time derivative vanishes, $\dot{F} = 0$. Consequently, F is a conserved quantity, i.e., it remains constant along the dynamical trajectories.

A system defined on a $2n$ -dimensional phase space is said to be *Liouville integrable* if there exist n functionally independent conserved quantities $\{F_1, \dots, F_n\}$, including the Hamiltonian H , which are all in mutual involution:

$$\{F_i, F_j\} = 0 \quad \forall i, j = 1, \dots, n. \quad (2.5)$$

According to *Liouville's theorem*, the equations of motion of such a system can be solved by quadratures.³ In particular, there exists a canonical transformation to so-called *action-angle variables*, in which the dynamics becomes particularly simple and transparent.⁴ This transformation takes the form

$$(q_i, p_i) \longrightarrow (F_i, \varphi_i), \quad (2.6)$$

where $\{F_i\}$ is the set of conserved action variables, and $\{\varphi_i\}$ are their conjugate angle variables. It then follows from Hamilton's equations that

$$\dot{F}_i = \{F_i, H\} = 0, \quad (2.7)$$

³One typically defines *quadratures* as solutions obtained by a finite sequence of algebraic operations and integrations.

⁴The terminology *action-angle variables* refers to the fact that the new variables consist of conserved quantities (actions) and their canonically conjugate cyclic variables (angles). These variables appear naturally in integrable systems.

$$\dot{\varphi}_i = \{\varphi_i, H\} \equiv \Omega_i, \quad (2.8)$$

where Ω_i are constant frequencies determined by the Hamiltonian. The general solution of the system in action-angle coordinates is then

$$F_i(t) = \alpha_i = \text{const.}, \quad (2.9)$$

$$\varphi_i(t) = \Omega_i t + \varphi_i(0), \quad (2.10)$$

showing that the motion is linear and uniform in the angle variables, while the actions remain constant in time.

Let us now consider two matrices L and M , referred to as the *Lax pair*, satisfying the Lax equation

$$\dot{L} = [M, L], \quad (2.11)$$

where $[\cdot, \cdot]$ denotes the matrix commutator.

It can be shown that this formulation implies the existence of conserved quantities Q_n , defined as

$$Q_n = \text{tr}(L^n), \quad (2.12)$$

which remain constant in time. These quantities are in involution and play a fundamental role in the integrability of the system. Let us prove that the quantities (2.12) are conserved under the Lax equation (2.11). We compute the time derivative of Q_n :

$$\frac{d}{dt} Q_n = \frac{d}{dt} \text{tr}(L^n) = \text{tr} \left(\frac{d}{dt} L^n \right). \quad (2.13)$$

Using the identity for the derivative of a matrix power:

$$\frac{d}{dt} L^n = \sum_{k=0}^{n-1} L^k \dot{L} L^{n-1-k},$$

one gets

$$\frac{d}{dt} Q_n = \text{tr} \left(\sum_{k=0}^{n-1} L^k \dot{L} L^{n-1-k} \right) = \sum_{k=0}^{n-1} \text{tr} \left(L^k [M, L] L^{n-1-k} \right). \quad (2.14)$$

Now let us use the cyclic property of the trace, $\text{tr}(AB) = \text{tr}(BA)$, and the fact that $\text{tr}([A, B]) = 0$ for any matrices A, B . Each term in the sum is a trace of a commutator:

$$\text{tr}(L^k [M, L] L^{n-1-k}) = \text{tr}([M, L] L^{n-1}) = \text{tr}([M, L^n]) = 0. \quad (2.15)$$

Therefore,

$$\frac{d}{dt} Q_n = 0,$$

which proves that $Q_n = \text{tr}(L^n)$ is conserved.

We can verify that equation (2.11) admits solutions of the form

$$L(t) = g(t)L(0)g(t)^{-1}, \quad M(t) = \frac{dg(t)}{dt}g(t)^{-1}, \quad (2.16)$$

where $g(t)$ is an invertible matrix-valued function of time. To confirm this, let us differentiate $L(t)$ with respect to time:

$$\begin{aligned} \dot{L}(t) &= \frac{d}{dt} [g(t)L(0)g(t)^{-1}] \\ &= \dot{g}(t)L(0)g(t)^{-1} + g(t)L(0)\frac{d}{dt}(g(t)^{-1}). \end{aligned} \quad (2.17)$$

We now use the identity

$$\frac{d}{dt}g(t)^{-1} = -g(t)^{-1}\dot{g}(t)g(t)^{-1},$$

to obtain

$$\begin{aligned} \dot{L}(t) &= \dot{g}(t)L(0)g(t)^{-1} - g(t)L(0)g(t)^{-1}\dot{g}(t)g(t)^{-1} \\ &= \dot{g}(t)g(t)^{-1} \cdot L(t) - L(t) \cdot \dot{g}(t)g(t)^{-1} \\ &= [\dot{g}(t)g(t)^{-1}, L(t)]. \end{aligned} \quad (2.18)$$

Finally, identifying $M(t) = \dot{g}(t)g(t)^{-1}$, we obtain

$$\dot{L}(t) = [M(t), L(t)], \quad (2.19)$$

which confirms that the ansatz (2.16) satisfies the Lax equation (2.11). This implies that the eigenvalues of the Lax matrix L are preserved under time evolution. Consequently, equation (2.11) is classified as an *isospectral flow*, reflecting the fact that the spectrum of L is invariant with respect to time.

Indeed, the term isospectral flow refers to a time evolution of a matrix (or more generally, a linear operator) such that its spectrum — the set of its eigenvalues — remains invariant in time. This concept naturally arises in the theory of integrable systems through the Lax pair formulation. A dynamical system admits a Lax representation if there exist matrices $L(t)$ and $M(t)$ such that the equations of motion can be written in the form (2.19). The structure of this equation ensures that $L(t)$ evolves by a similarity transformation:

$$L(t) = g(t)L(0)g(t)^{-1}, \quad (2.20)$$

for some invertible matrix $g(t)$. As similarity transformations preserve the spectrum of a matrix, it follows that all eigenvalues of $L(t)$ are conserved quantities. Isospectral flows play a fundamental role in integrable systems, as the conserved quantities — which guarantee integrability in the sense of Liouville — are often encoded in the eigenvalues of the Lax matrix L .⁵

⁵In the Lax pair formulation of integrable systems, the conserved quantities are always encoded in the eigenvalues of the Lax matrix L , since the isospectral condition $\dot{L} = [M, L]$ ensures that these eigenvalues remain constant in time. Thus, functions of the spectrum, such as $\text{tr } L^n$, yield conserved quantities. However, in more general settings, additional or alternative conserved quantities may arise from *monodromy* or *transfer matrices*, and not all integrable systems necessarily admit a Lax representation with this property.

Let us define the *Kronecker product* of two $n \times n$ matrices A and B . The Kronecker product $A \otimes B$ is given by

$$A \otimes B = \begin{pmatrix} a_{11}B & a_{12}B & \cdots & a_{1n}B \\ a_{21}B & a_{22}B & \cdots & a_{2n}B \\ \vdots & \vdots & \ddots & \vdots \\ a_{n1}B & a_{n2}B & \cdots & a_{nn}B \end{pmatrix} = \begin{pmatrix} a_{11}b_{11} & a_{11}b_{12} & \cdots & a_{1n}b_{1n} \\ a_{11}b_{21} & a_{11}b_{22} & \cdots & a_{1n}b_{2n} \\ \vdots & \vdots & \ddots & \vdots \\ a_{n1}b_{n1} & a_{n1}b_{n2} & \cdots & a_{nn}b_{nn} \end{pmatrix}. \quad (2.21)$$

This operation produces a block matrix where each entry a_{ij} of A is multiplied by the entire matrix B .

Let us now consider the tensor product space $V^{\otimes N} = V \otimes V \otimes \cdots \otimes V$, consisting of N copies of the vector space V . We introduce the notation A_i to indicate that the operator A acts non-trivially only on the i -th site and as the identity elsewhere. That is,

$$A_i = \mathbb{I}^{\otimes(i-1)} \otimes A \otimes \mathbb{I}^{\otimes(N-i)}, \quad (2.22)$$

where \mathbb{I} is the identity operator on V .

From this definition, it is straightforward to verify that two operators acting on different sites commute:

$$i \neq j \Rightarrow [A_i, A_j] = 0. \quad (2.23)$$

This construction allows us to naturally define a matrix L_1 in the extended space as

$$L_1 = L \otimes \mathbb{I}, \quad (2.24)$$

where L acts on the first copy of V , and \mathbb{I} acts on an auxiliary or second space.

Let us now assume that the Lax matrix L can be diagonalized by a similarity transformation using some invertible matrix U :

$$L = U \Lambda U^{-1}, \quad (2.25)$$

where Λ is a diagonal matrix. This implies that the eigenvalues Λ_{ii} are conserved quantities, and hence

$$\{\Lambda_i, \Lambda_j\} = 0, \quad \forall i, j, \quad (2.26)$$

where the indices i and j label the sites, consistent with the notation introduced in equation (2.22).

Using this property, we can express the Poisson bracket $\{L_1, L_2\}$ by substituting the decomposed forms:

$$L_1 = U_1 \Lambda_1 U_1^{-1}, \quad L_2 = U_2 \Lambda_2 U_2^{-1}. \quad (2.27)$$

As shown in appendix A, this leads to the following fundamental Poisson bracket relation:

$$\{L_1, L_2\} = [r_{12}, L_1] - [r_{21}, L_2], \quad (2.28)$$

where r_{12} is known as the classical r –matrix.

We can now insert this result into the Jacobi identity involving a triple of Lax matrices $\{L_1, L_2, L_3\}$, which yields:

$$\begin{aligned} & [L_1, \{L_2, r_{13}\} - \{L_3, r_{12}\} + [r_{12}, r_{13} + r_{23}] + [r_{32}, r_{13}]] + \\ & [L_2, \{L_3, r_{21}\} - \{L_1, r_{23}\} + [r_{23}, r_{21} + r_{31}] + [r_{13}, r_{21}]] + \\ & [L_3, \{L_1, r_{32}\} - \{L_2, r_{31}\} + [r_{31}, r_{32} + r_{12}] + [r_{21}, r_{32}]] = 0. \end{aligned} \quad (2.29)$$

In the special case where the r –matrices are independent of the dynamical variables and antisymmetric, i.e., $r_{ij} = -r_{ji}$, the above expression simplifies and leads to the celebrated *classical Yang–Baxter equation* (CYBE):

$$[r_{12}, r_{13} + r_{23}] + [r_{32}, r_{13}] = 0. \quad (2.30)$$

This structure is central to the classical r –matrix formalism and underlies many integrable systems.

As a conclusion to our discussion of classical integrability, we summarize the key features of the classical r –matrix formalism.

Summary of the classical r –matrix formalism. The classical r –matrix formalism provides a powerful algebraic framework for studying integrable systems in the Hamiltonian formulation. It encodes the Poisson bracket relations between the elements of the Lax matrix and ensures the integrability of the model via the existence of conserved quantities in involution.

Let L be the Lax matrix of a classical integrable system. To describe its Poisson algebraic structure, we introduce the tensor product notation:

$$L_1 = L \otimes \mathbb{I}, \quad L_2 = \mathbb{I} \otimes L, \quad (2.31)$$

The Poisson brackets of the matrix elements of L can be compactly written using an object called the classical r –matrix, denoted by $r_{12}(u, v) \in \text{End}(V \otimes V)$, satisfying

$$\{L_1(u), L_2(v)\} = [r_{12}(u, v), L_1(u)] - [r_{21}(u, v), L_2(v)], \quad (2.32)$$

where u, v are spectral parameters and $r_{21}(u, v) \equiv P r_{12}(v, u) P$, with P being the permutation operator on $V \otimes V$.

Isospectrality and integrals of motion. From the structure of (2.32), it follows that the traces $\text{tr}(L^n(u))$ form a commuting family of conserved quantities:

$$\{\text{tr}(L^n(u)), \text{tr}(L^m(v))\} = 0 \quad \forall m, n. \quad (2.33)$$

Thus, the existence of an r –matrix satisfying (2.32) guarantees Liouville integrability of the system.

Classical Yang–Baxter equation. The consistency of this Poisson structure is ensured by the classical Yang–Baxter equation:

$$[r_{12}, r_{13}] + [r_{12}, r_{23}] + [r_{13}, r_{23}] = 0 \in \text{End}(V^{\otimes 3}), \quad (2.34)$$

which the r -matrix must satisfy.

2.2 Quantum integrability

For quantum integrability, we assume the existence of a family of mutually commuting conserved charges Q_i ,

$$[Q_i, Q_j] = 0, \quad i, j = 1, 2, \dots. \quad (2.35)$$

Our task is to construct these charges from the underlying integrable structure.

To this end, we introduce a quantum R -matrix, an operator

$$R(z_1, z_2) : \text{End}(\mathcal{H} \otimes \mathcal{H}) \longrightarrow \text{End}(\mathcal{H} \otimes \mathcal{H}), \quad (2.36)$$

which satisfies the *quantum Yang–Baxter equation* (QYBE):

$$R_{12}(z_1, z_2) R_{13}(z_1, z_3) R_{23}(z_2, z_3) = R_{23}(z_2, z_3) R_{13}(z_1, z_3) R_{12}(z_1, z_2), \quad (2.37)$$

with spectral parameters $z_i \in \mathbb{C}$. We will restrict to the additive case

$$R_{ij}(z_i, z_j) = R_{ij}(z_i - z_j). \quad (2.38)$$

Shifting $z_1 \rightarrow z_1 + z_3$ and $z_2 \rightarrow z_2 + z_3$ then yields the more familiar form

$$R_{12}(z_1 - z_2) R_{13}(z_1) R_{23}(z_2) = R_{23}(z_2) R_{13}(z_1) R_{12}(z_1 - z_2). \quad (2.39)$$

Next, we introduce a Lax operator \mathcal{L}_i that relates the state at site i to the state at site $i + 1$:

$$|v_{i+1}\rangle = \mathcal{L}_i |v_i\rangle. \quad (2.40)$$

Equivalently, \mathcal{L}_i satisfies the RLL relation

$$R_{\alpha\beta}(z_\alpha - z_\beta) \mathcal{L}_{\alpha j}(z_\alpha) \mathcal{L}_{\beta j}(z_\beta) = \mathcal{L}_{\beta j}(z_\beta) \mathcal{L}_{\alpha j}(z_\alpha) R_{\alpha\beta}(z_\alpha - z_\beta), \quad (2.41)$$

where $\mathcal{L}_{\alpha j}(z)$ acts on the tensor product $\mathcal{V}_\alpha \otimes \mathcal{H}_j$, with \mathcal{V}_α the auxiliary space (labeled by α) and \mathcal{H}_j the physical Hilbert space at site j .

For a fixed R -matrix, the RLL equation generally admits multiple solutions for the Lax operator $\mathcal{L}(z)$. A canonical solution is simply

$$\mathcal{L}(z) = R(z), \quad (2.42)$$

which we adopt for concreteness in what follows.

We next assemble the Lax operators into the *monodromy matrix*, which transports states from site 1 to site N :

$$\mathcal{T}_\alpha(z) = \mathcal{L}_{\alpha N}(z) \mathcal{L}_{\alpha N-1}(z) \cdots \mathcal{L}_{\alpha 2}(z) \mathcal{L}_{\alpha 1}(z). \quad (2.43)$$

One shows, using repeated applications of the RLL relation, that \mathcal{T} satisfies

$$R_{\alpha\beta}(z_\alpha - z_\beta) \mathcal{T}_\alpha(z_\alpha) \mathcal{T}_\beta(z_\beta) = \mathcal{T}_\beta(z_\beta) \mathcal{T}_\alpha(z_\alpha) R_{\alpha\beta}(z_\alpha - z_\beta). \quad (2.44)$$

Taking the trace over the auxiliary space \mathcal{V}_α defines the *transfer matrix*

$$t(z) = \text{tr}_\alpha \mathcal{T}_\alpha(z), \quad (2.45)$$

which generates the mutually commuting conserved charges. Indeed, cyclicity of the trace implies

$$[t(z_1), t(z_2)] = 0 \quad \forall z_1, z_2. \quad (2.46)$$

Expanding its logarithm in powers of z ,

$$\log t(z) = \sum_{\ell=0}^{\infty} Q_\ell z^\ell, \quad (2.47)$$

we identify

$$Q_\ell = \frac{1}{\ell!} \left. \frac{d^\ell}{dz^\ell} \log t(z) \right|_{z=0}, \quad \ell = 0, 1, 2, \dots, \quad (2.48)$$

so that knowledge of the R -matrix determines $t(z)$ and hence all conserved charges Q_ℓ .

2.3 Algebraic Bethe ansatz

Rather than constructing each conserved charge individually, one can diagonalize the transfer matrix:

$$t(z) |\Lambda\rangle = \Lambda(z) |\Lambda\rangle, \quad (2.49)$$

where $|\Lambda\rangle$ is an eigenvector of $t(z)$ and $\Lambda(z)$ its eigenvalue. The eigenvalues of all charges Q_{n+1} then follow from the expansion

$$\log \Lambda(z) = \sum_{n=0}^{\infty} \Lambda^{(Q_{n+1})} z^n \Rightarrow \Lambda^{(Q_{n+1})} = \frac{1}{n!} \left. \frac{d^n}{dz^n} \log \Lambda(z) \right|_{z=0}. \quad (2.50)$$

This diagonalization procedure, known as the *algebraic Bethe ansatz* (ABA), is especially powerful: it circumvents the exponential growth of the Hamiltonian matrix in site number by exploiting the integrable structure encoded in $t(z)$.

We decompose the monodromy matrix $\mathcal{T}_\alpha(z)$ as

$$\mathcal{T}_\alpha(z) = \mathcal{L}_{\alpha N}(z) \mathcal{L}_{\alpha N-1}(z) \cdots \mathcal{L}_{\alpha 1}(z) = \begin{pmatrix} \mathcal{A}(z) & \mathcal{B}(z) \\ \mathcal{C}(z) & \mathcal{D}(z) \end{pmatrix}, \quad (2.51)$$

where $\mathcal{A}, \mathcal{B}, \mathcal{C}, \mathcal{D}$ act on the physical Hilbert space $\mathcal{H}^{\otimes N}$ (of dimension 2^N). The transfer matrix is then

$$t(z) = \text{tr}_\alpha \mathcal{T}_\alpha(z) = \mathcal{A}(z) + \mathcal{D}(z). \quad (2.52)$$

Consider the ferromagnetic pseudo-vacuum

$$|0\rangle = \bigotimes_{j=1}^N \begin{pmatrix} 1 \\ 0 \end{pmatrix}_j, \quad (2.53)$$

which satisfies

$$\mathcal{C}(z)|0\rangle = 0, \quad \mathcal{A}(z)|0\rangle = a(z)|0\rangle, \quad \mathcal{D}(z)|0\rangle = d(z)|0\rangle. \quad (2.54)$$

Only the operator $\mathcal{B}(z)$ creates excitations on $|0\rangle$. We define the *Bethe states*

$$|\{z_i\}\rangle = \mathcal{B}(z_1)\mathcal{B}(z_2)\cdots\mathcal{B}(z_m)|0\rangle. \quad (2.55)$$

For generic parameters $\{z_i\}$, these are off-shell states; imposing the Bethe equations on $\{z_i\}$ ensures that $|\{z_i\}\rangle$ becomes an eigenvector of $t(z)$.

We start from

$$t(z)|\Lambda(z_1, \dots, z_m)\rangle = [\mathcal{A}(z) + \mathcal{D}(z)]\mathcal{B}(z_1)\mathcal{B}(z_2)\cdots\mathcal{B}(z_m)|0\rangle. \quad (2.56)$$

Using the RTT commutation relations, one moves $\mathcal{A}(z)$ and $\mathcal{D}(z)$ past the $\mathcal{B}(z_i)$ operators and evaluates their action on $|0\rangle$. One then obtains

$$\begin{aligned} t(z)\mathcal{B}(z_1)\cdots\mathcal{B}(z_m)|0\rangle &= \Lambda(z; \{z_i\})\mathcal{B}(z_1)\cdots\mathcal{B}(z_m)|0\rangle \\ &+ \sum_{i=1}^m \left[\mathcal{M}_i^{(A)}(z; \{z_j\}) + \mathcal{M}_i^{(D)}(z; \{z_j\}) \right] \mathcal{B}(z_1)\cdots\widehat{\mathcal{B}(z_i)}\cdots\mathcal{B}(z_m)|0\rangle, \end{aligned} \quad (2.57)$$

where $\widehat{\mathcal{B}(z_i)}$ indicates omission of the i -th \mathcal{B} operator. The functions $\mathcal{M}_i^{(A,D)}$ arise from commutators with \mathcal{A} and \mathcal{D} .

Requiring that all unwanted terms vanish determines the *Bethe roots* $\{z_i\}$ through

$$\mathcal{M}_i^{(A)}(z; \{z_j\}) + \mathcal{M}_i^{(D)}(z; \{z_j\}) = 0 \quad \text{for } i = 1, \dots, m. \quad (2.58)$$

When these *Bethe equations* are satisfied, the second line disappears and $|\{z_i\}\rangle$ becomes an eigenstate of the transfer matrix with eigenvalue $\Lambda(z; \{z_i\})$.

3 Richardson–Gaudin models and Bethe equations

3.1 The Richardson model

We consider a system of fermions interacting via a reduced BCS (rBCS) Hamiltonian of the form:

$$H_{\text{rBCS}} = \sum_{j,\sigma} \epsilon_j c_{j\sigma}^\dagger c_{j\sigma} - g \sum_{i,j} c_{i+}^\dagger c_{i-}^\dagger c_{j-} c_{j+}, \quad (3.1)$$

where ϵ_j denotes the single particle energy level j ($j = 1, \dots, L$), $g > 0$ is the coupling constant, and $c_{j\sigma}^\dagger$, $c_{j\sigma}$ are fermionic creation and annihilation operators with $\sigma = +, -$ labeling time-reversed states.

When $g = 0$, electrons occupy single particle levels independently. A Cooper pair consisting of two electrons in time-reversed states $|\pm\rangle$ contributes an energy $2\epsilon_j$. For a general system with a given set \mathcal{S} of N electrons, one can decompose the Hilbert space into two subspaces according to the underlying pairing structure. Specifically, let us denote (i) a paired subset $\mathcal{U} \subset \mathcal{S}$, with $2M$ electrons forming M Cooper pairs; (ii) a blocked subset $\mathcal{B} = \mathcal{S} \setminus \mathcal{U}$, consisting of $K = N - 2M$ unpaired electrons. This decomposition of the Hilbert space allows us to restrict the dynamics to the paired sector \mathcal{U} , where the reduced BCS Hamiltonian acts nontrivially. The corresponding state vector can be factorized as

$$|M, K\rangle = \prod_{i \in \mathcal{B}} c_{i\sigma}^\dagger |\Psi_M\rangle_{\mathcal{U}}, \quad (3.2)$$

where $|\Psi_M\rangle_{\mathcal{U}}$ describes the wavefunction of the M Cooper pairs, and the product over \mathcal{B} creates the blocked single particle excitations. Since the singly occupied states do not participate in pairing, their total energy is simply additive:

$$\mathbb{E}_{\mathcal{B}} = \sum_{i \in \mathcal{B}} \epsilon_i = \sum_{i=1}^K \epsilon_i \equiv \mathbb{E}(K). \quad (3.3)$$

By focusing on the subspace associated with \mathcal{U} , one can solve the eigenvalue problem for the paired sector independently, using the exact Bethe ansatz methods described in the following subsections.

Hard–core boson representation. We define pair creation and annihilation operators as

$$b_j^\dagger = c_{j+}^\dagger c_{j-}^\dagger, \quad b_j = c_{j-} - c_{j+}, \quad (3.4)$$

which obey the following commutation relations:

$$b_j^{\dagger 2} = 0, \quad [b_i, b_j^\dagger] = \delta_{ij}(1 - 2b_j^\dagger b_j), \quad [b_j^\dagger b_j, b_k^\dagger] = \delta_{jk} b_j^\dagger \quad (3.5)$$

(see appendix B). These reflect the fermionic nature of the underlying electrons and define the so-called *hard-core boson* algebra.

In this representation, the Hamiltonian acting on the paired subspace \mathcal{U} becomes:

$$H_{\mathcal{U}} = \sum_{j \in \mathcal{U}} 2\epsilon_j b_j^\dagger b_j - g \sum_{i, j \in \mathcal{U}} b_i^\dagger b_j. \quad (3.6)$$

The factor of 2 in the Hamiltonian appears because each Cooper pair is made of two electrons. When there is no interaction ($g = 0$), both electrons occupy the same energy level ϵ_j . Each one contributes ϵ_j to the total energy, so the pair together contributes $2\epsilon_j$. For this reason, we treat the energy level of a Cooper pair as $2\epsilon_j$.

Indeed, let us start from the single particle energy term for level j :

$$\sum_{\sigma} \epsilon_j c_{j\sigma}^{\dagger} c_{j\sigma} = \epsilon_j (c_{j+}^{\dagger} c_{j+} + c_{j-}^{\dagger} c_{j-}). \quad (3.7)$$

We now employ the definition of the pair creation operator $b_j^{\dagger} = c_{j+}^{\dagger} c_{j-}^{\dagger}$, and define the pair number operator as $b_j^{\dagger} b_j$. In the subspace where level j is either empty or doubly occupied by a Cooper pair, we have:⁶

$$c_{j+}^{\dagger} c_{j+} + c_{j-}^{\dagger} c_{j-} = 2b_j^{\dagger} b_j, \quad (3.8)$$

and thus

$$\sum_{\sigma} \epsilon_j c_{j\sigma}^{\dagger} c_{j\sigma} = 2\epsilon_j b_j^{\dagger} b_j. \quad (3.9)$$

This step holds under the assumption that the Hilbert space is restricted to states where each energy level is either unoccupied or occupied by a full Cooper pair. That is, singly occupied states are excluded. This is the standard assumption in the reduced BCS model, which focuses solely on the dynamics of paired electrons. Outside of this subspace, the relation does not hold.

Bethe ansatz and Richardson equations. We seek eigenstates of the form:

$$|\Psi_M\rangle_{\mathcal{U}} = \prod_{\nu=1}^M B_{\nu}^{\dagger} |0\rangle \quad \text{with} \quad B_{\nu}^{\dagger} = \sum_{j \in \mathcal{U}} \frac{b_j^{\dagger}}{2\epsilon_j - E_{\nu}}, \quad (3.10)$$

where E_{ν} is a spectral parameter associated with the ν -th Cooper pair. The total energy of the system is then

$$\mathbb{E}(M) = \sum_{\nu=1}^M E_{\nu}. \quad (3.11)$$

Introducing the collective operator

$$B_0^{\dagger} = \sum_{j \in \mathcal{U}} b_j^{\dagger}, \quad (3.12)$$

we rewrite the Hamiltonian (3.6) as

$$H_{\mathcal{U}} = \sum_{j \in \mathcal{U}} 2\epsilon_j b_j^{\dagger} b_j - g B_0^{\dagger} B_0. \quad (3.13)$$

⁶If level j is doubly occupied, then $c_{j+}^{\dagger} c_{j+} = 1$ and $c_{j-}^{\dagger} c_{j-} = 1$, so $\epsilon_j(1+1) = 2\epsilon_j$. In this case, $b_j^{\dagger} b_j = 1$, and thus the right-hand side is $2\epsilon_j b_j^{\dagger} b_j$. If level j is empty, all number operators vanish, and so does $b_j^{\dagger} b_j$, making both sides zero. Therefore, the equality

$$\epsilon_j (c_{j+}^{\dagger} c_{j+} + c_{j-}^{\dagger} c_{j-}) = 2\epsilon_j b_j^{\dagger} b_j$$

holds when restricted to the subspace where single occupancy does not occur.

Applying $H_{\mathcal{U}}$ to the ansatz state and simplifying using algebra detailed in appendix C, we find:

$$H_{\mathcal{U}} |\Psi_M\rangle_{\mathcal{U}} = \mathbb{E}(M) |\Psi_M\rangle_{\mathcal{U}} + \sum_{\nu=1}^M \left\{ 1 - g \sum_{j \in \mathcal{U}} \frac{1}{2\epsilon_j - E_{\nu}} + 2g \sum_{\mu \neq \nu} \frac{1}{E_{\mu} - E_{\nu}} \right\} \times B_0^{\dagger} \prod_{\eta \neq \nu} B_{\eta}^{\dagger} |0\rangle. \quad (3.14)$$

For $|\Psi_M\rangle_{\mathcal{U}}$ to be a true eigenstate, the second term must vanish. This yields a set of coupled nonlinear equations, known as the *Richardson equations*:

$$\frac{1}{g} - \sum_{j=1}^L \frac{1}{2\epsilon_j - E_{\nu}} + \sum_{\mu=1(\neq \nu)}^M \frac{2}{E_{\mu} - E_{\nu}} = 0, \quad \forall \nu = 1, \dots, M.$$

(3.15)

These equations determine the allowed values of E_{ν} , which in turn define the exact energy spectrum and eigenstates of the reduced BCS Hamiltonian.

3.2 Gaudin spin models and the conserved charges of the Richardson model

There exists a profound connection between the Richardson reduced BCS model and a class of quantum integrable spin systems (*spin chains*) known as *Gaudin models* [5, 6]. These models are constructed from a given Lie algebra—typically $\mathfrak{sl}(2, \mathbb{C})$ —but the formalism extends naturally to other semisimple Lie algebras. A key feature of Gaudin models is the existence of mutually commuting Hamiltonians derived from the algebraic structure, governing the integrable dynamics of the system.

Let \mathfrak{g} be a semisimple Lie algebra of dimension d , and consider L distinct complex parameters $z_i \in \mathbb{C}$. The Gaudin Hamiltonians are defined as

$$H_{\mathfrak{g},i} = \sum_{j \neq i} \sum_{a=1}^d \frac{I_a^{(i)} I^{a(j)}}{z_i - z_j}, \quad (3.16)$$

where $\{I_a\}$ is a basis of \mathfrak{g} , and $\{I^a\}$ is its dual with respect to an invariant scalar product (typically the Killing form). These Hamiltonians act on the tensor product space

$$\mathcal{V}_{\lambda} \equiv \mathcal{V}_{\lambda_1} \otimes \cdots \otimes \mathcal{V}_{\lambda_L},$$

where each \mathcal{V}_{λ_i} is a finite-dimensional irreducible representation of \mathfrak{g} , labeled by a dominant weight λ_i . The operator $I_a^{(i)}$ acts nontrivially on the i -th tensor component and trivially on all others.

A central problem in the theory of Gaudin models is the simultaneous diagonalization of the commuting Hamiltonians $H_{\mathfrak{g},i}$, which can be achieved via the algebraic Bethe ansatz originally introduced by Gaudin.

The $\mathfrak{su}(2)$ Gaudin model and the Richardson equations. In the context of the Richardson model, the relevant Gaudin model is associated with the $\mathfrak{su}(2)$ algebra. The Hamiltonians take the form

$$H_{\mathfrak{su}(2),i} = \sum_{j \neq i} \frac{1}{\epsilon_i - \epsilon_j} \left[S_i^z S_j^z + \frac{1}{2} (S_i^+ S_j^- + S_i^- S_j^+) \right] \equiv \sum_{j \neq i} \frac{\mathbf{S}_i \cdot \mathbf{S}_j}{\epsilon_i - \epsilon_j}, \quad (3.17)$$

where the $\mathfrak{su}(2)$ generators are realized via hard-core boson operators:

$$S_j^+ = b_j^\dagger, \quad S_j^- = b_j, \quad S_j^z = \frac{1}{2} - \hat{N}_j,$$

with $\hat{N}_j = b_j^\dagger b_j$ as the pair number operator. These Hamiltonians can be diagonalized using the Richardson–Bethe ansatz. The corresponding energy eigenvalues are

$$\mathbb{E}_{\mathfrak{su}(2)}(M) = \sum_{\nu=1}^M E_\nu, \quad (3.18)$$

where the parameters E_ν satisfy the Richardson equations (3.15) in the limit $g \rightarrow \infty$.

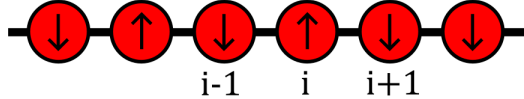


Figure 1. The $\mathfrak{su}(2)$ Gaudin model describes a one-dimensional quantum spin system with long-range, position-dependent interactions. Each site i in the chain hosts a spin- $\frac{1}{2}$ particle, represented by the generators $\mathbf{S}_i = (S_i^+, S_i^-, S_i^z)$ of the Lie algebra $\mathfrak{su}(2)$. The interactions between spins are governed by a set of mutually commuting Hamiltonians (3.17), in which the coupling strengths depend on the parameters ϵ_i , which can be interpreted as position-like inhomogeneity parameters assigned to each site. These parameters introduce non-uniform interaction strengths of the form $1/(\epsilon_i - \epsilon_j)$, leading to an integrable deformation of the uniform spin chain. In this framework, the Bethe roots E_ν arise as solutions to the Richardson (Bethe ansatz) equations in the limit $g \rightarrow \infty$ and carry a clear physical meaning: each E_ν corresponds to a collective excitation of the spin system. The total energy of an eigenstate is obtained as the sum over all Bethe roots (3.18) where M is the number of such collective excitations.

Conserved quantities and the rBCS Hamiltonian. The rational Gaudin Hamiltonians (3.17) naturally appear in the definition of conserved quantities of the rBCS model, known as the Cambiaggio–Rivas–Saraceno (CRS) integrals of motion [14]:

$$R_i = -S_i^z - g H_{\mathfrak{su}(2),i} = -S_i^z - g \sum_{j \neq i} \frac{\mathbf{S}_i \cdot \mathbf{S}_j}{\epsilon_i - \epsilon_j}, \quad i = 1, \dots, L. \quad (3.19)$$

These operators commute with each other and with the rBCS Hamiltonian. This allows the Hamiltonian to be re-expressed as [7, 14]:

$$H_{\text{rBCS}} = H_{\text{XY}} + \sum_{j=1}^L \epsilon_j + g \left(\frac{1}{2} L - M \right), \quad (3.20)$$

$$H_{XY} = \sum_{j=1}^L 2\epsilon_j R_j + g \left(\sum_{j=1}^L R_j \right)^2 - \frac{3}{4} g L. \quad (3.21)$$

Hence, an alternative strategy to find the spectrum of H_{rBCS} is to solve the eigenproblems for the quantum integrals of motion R_i .

Connection to the central spin model. Each CRS operator R_i can be interpreted as a Hamiltonian of the *central spin model* (or *Gaudin magnet*), where a central spin \mathbf{S}_0 interacts with a bath of L surrounding spins \mathbf{S}_j :

$$H_{\text{cs}} \equiv B R_{i=0} = -B S_0^z + \sum_{j=1}^L A_j \mathbf{S}_0 \cdot \mathbf{S}_j. \quad (3.22)$$

The magnetic field B and inhomogeneous couplings A_j are parametrized to match the Richardson model:

$$B = -\frac{2}{g}, \quad A_j = \frac{2}{\epsilon_0 - \epsilon_j}.$$

When $\epsilon_0 = 0$, the parameters ϵ_j coincide with the energy levels of the rBCS model.

Eigenvalues of the conserved charges and the Yang–Yang function. A closed form expression for the eigenvalues λ_i of the conserved charges R_i was obtained by Sierra [7] using techniques from two-dimensional conformal field theory (see subsection 3.3):

$$\lambda_i = \frac{g}{2} \left. \frac{\partial \mathcal{W}_{\text{crit}}^{\text{R}}(\mathbf{z}, \mathbf{E}^{\text{c}})}{\partial z_i} \right|_{z_i=2\epsilon_i} = -\frac{1}{2} + g \left(\sum_{\nu=1}^M \frac{1}{2\epsilon_i - E_{\nu}^{\text{c}}} - \frac{1}{4} \sum_{j \neq i}^L \frac{1}{\epsilon_i - \epsilon_j} \right). \quad (3.23)$$

Here, $\mathbf{E}^{\text{c}} = \{E_1^{\text{c}}, \dots, E_M^{\text{c}}\}$ is a solution of the Richardson equations, and $\mathcal{W}_{\text{crit}}^{\text{R}}$ is the critical value of the YY function:

$$\begin{aligned} \mathcal{W}^{\text{R}}(\mathbf{z}, \mathbf{E}) = & - \sum_{i < j}^L \log(z_i - z_j) - 4 \sum_{\nu < \mu}^M \log(E_{\nu} - E_{\mu}) \\ & + 2 \sum_{i=1}^L \sum_{\nu=1}^M \log(z_i - E_{\nu}) + \frac{1}{g} \left(- \sum_{i=1}^L z_i + 2 \sum_{\nu=1}^M E_{\nu} \right). \end{aligned} \quad (3.24)$$

The conditions $\partial \mathcal{W}^{\text{R}} / \partial E_{\nu} = 0$, $\nu = 1, \dots, M$ recover the Richardson equations, confirming that \mathcal{W}^{R} acts as a potential function for the Bethe ansatz equations.

Thus, an alternative formulation of the Richardson–Gaudin spectral problem involves the YY function (3.24) (or functional, if the E_{ν} are interpreted as functions of the coupling g), whose stationary conditions reproduce the Richardson equations. This variational perspective not only provides a powerful numerical target—minimizing \mathcal{W}^{R} via gradient-based methods⁷—but also underlies an elegant electrostatic analogy: the rapidities E_{ν} behave like unit “charges” on the complex plane, repelling one another and attracted to fixed “background” charges at the single particle energies ϵ_j .

⁷See the conclusions for further details.

3.3 Realization via 2D conformal field theory

The exact Richardson solution admits an interpretation in terms of conformal blocks of a two-dimensional conformal field theory. In particular, to solve the eigenproblem for the Richardson conserved charges, Sierra [7] showed that the Knizhnik–Zamolodchikov (KZ) equation for the $\widehat{\mathfrak{su}(2)_k}$ WZW block,

$$\left(\kappa \partial_{z_i} - \sum_{\substack{j=1 \\ j \neq i}}^{L+1} \frac{\mathbf{S}_i \cdot \mathbf{S}_j}{z_i - z_j} \right) \psi^{\text{WZW}}(z_1, \dots, z_{L+1}) = 0, \quad \kappa = \frac{k+2}{2}, \quad (3.25)$$

is entirely equivalent to the eigenvalue equation:

$$\frac{1}{2g} R_i \psi = -\kappa \partial_{z_i} \psi, \quad \psi^{\text{WZW}} = \exp[(2g\kappa)^{-1} H_{\text{XY}}] \psi. \quad (3.26)$$

Here, $\psi \equiv \psi_{\mathbf{m}}^{\text{CG}}(\mathbf{z})$ denotes a perturbed WZW conformal block in the free field (Coulomb gas) representation. More precisely, $\psi_{\mathbf{m}}^{\text{CG}}(\mathbf{z})$ consists of

- i. the $\widehat{\mathfrak{su}(2)_k}$ WZW chiral primary fields $\Phi_m^j(z) = (\gamma(z))^{j-m} V_\alpha(z)$ built out of the γ -field of the $\beta\gamma$ -system and Virasoro chiral vertex operators $V_{\Delta_\alpha}(z)$, $\Delta_\alpha = \alpha(\alpha - 2\alpha_0) = j(j+1)/(k+2)$ represented as normal ordered exponentials of the free field $\phi(z)$.⁸
- ii. WZW screening charges:

$$Q = \oint_C \frac{dE}{2\pi i} S(E), \quad S(E) = \beta(E) V_{2\alpha_0}(E);$$

- iii. the operator

$$V_g = \exp \left[-\frac{i\alpha_0}{g} \oint_{C_g} dz z \partial_z \phi(z) \right],$$

which breaks conformal invariance.

Within this realization to every energy level $z_i = 2\epsilon_i$ corresponds the field $\Phi_{m_i}^j(z_i)$ with the spin $j = \frac{1}{2}$ and the “third component” $m_i = \frac{1}{2}$ (or $m_i = -\frac{1}{2}$) if the corresponding energy level is empty (or occupied) by a pair of fermions. Integration variables E_ν in screening operators are the Richardson parameters. The operator V_g implements the coupling g and is a source of the term $\frac{1}{g}$ in the Richardson equations (3.15).

After ordering, $\psi_{\mathbf{m}}^{\text{CG}}(\mathbf{z})$ has a structure of a multidimensional contour integral,

$$\psi_{\mathbf{m}}^{\text{CG}}(\mathbf{z}) = \oint_{C_1} dE_1 \dots \oint_{C_M} dE_M \psi_{\mathbf{m}}^{\beta\gamma}(\mathbf{z}, \mathbf{E}) e^{-\alpha_0^2 \mathcal{W}^R(\mathbf{z}, \mathbf{E})}, \quad (3.27)$$

⁸Here, $\alpha = (k+2)^{-\frac{1}{2}} j = -2\alpha_0 j$.

where $\mathcal{W}^R(\mathbf{z}, \mathbf{E})$ is given by (3.24). In the limit $\alpha_0 \rightarrow \infty \Leftrightarrow k \rightarrow -2 \Leftrightarrow \kappa \rightarrow 0$, this integral can be calculated using the saddle point method. The stationary solutions are then given by the solutions of the Richardson equations. After all one gets

$$\psi_{\mathbf{m}}^{\text{CG}}(\mathbf{z}) \sim \psi^R e^{-\alpha_0^2 \mathcal{W}_{\text{crit}}^R(\mathbf{z}, \mathbf{E}^c)} \quad \text{for } \alpha_0 \rightarrow \infty, \quad (3.28)$$

where $\psi^R \equiv \psi_{\mathbf{m}}^{\beta\gamma}(\mathbf{z}, \mathbf{E}^c)$ is the Richardson wave function. Using this asymptotic limit to the equation (3.26) one obtains $R_i \psi^R = \lambda_i \psi^R$ for $\kappa \rightarrow 0$, where λ_i are given by (3.23).

Yang–Yang function via Gaiotto–Witten irregular conformal blocks. The subsequent points represent novel findings beyond those in [7]. The saddle-point asymptotic in (3.28) is exactly the large- c limit of the conformal blocks.⁹ More generally, in this limit the saddle values of the Coulomb gas integrals—i.e., the critical values $\mathcal{W}_{\text{crit}}$ of the YY functions—coincide with the exponentiated classical conformal blocks, which in turn admit independent power series expansions. Since finding $\mathcal{W}_{\text{crit}}$ normally requires solving the Bethe (saddle-point) equations, one can instead approximate it by truncating the series for the classical block. In subsection 6.4, we present a concrete example: the Dotsenko–Fateev integral representation of the Virasoro four-point conformal block on the sphere. In the classical (saddle-point) limit, its saddle-point equations reduce to a Gaudin-type system.

The construction of the function $\mathcal{W}_{\text{crit}}^R$ in [7]—which both generates the full spectrum of conserved charges in the Richardson model and solves the eigenvalue problem for the Gaudin magnet (central spin) Hamiltonian—reveals a deep link between quantum integrability, conformal symmetry, and the physics of Richardson–Gaudin models. However, because this construction explicitly breaks conformal invariance, one cannot directly invoke standard 2D CFT machinery (e.g., factorization over a complete basis of intermediate states) to compute conformal blocks or their power series coefficients—though a perturbed CFT approach might still apply. Remarkably, one can reformulate the YY function for RG models in a manner that preserves conformal symmetry and permits the use of all standard techniques of two-dimensional conformal field theory.

The YY function (3.24) also emerges in a setting far removed from conventional quantum integrability. In their study of a four-dimensional gauge-theoretic approach to the Jones polynomial, Gaiotto and Witten [17] recognized that the relevant saddle-point equations coincide with the Bethe ansatz system (3.15). Moreover, Gaiotto and Witten exhibited a free field realization of the associated YY function in terms of irregular, degenerate Virasoro conformal blocks. Their construction uses the usual degenerate vertex operators and screening charges together with a rank-one irregular insertion at infinity, which creates the corresponding irregular state from the vacuum.¹⁰

⁹Here, $c = 3 - 12\alpha_0^2 = 3k/(k+2)$.

¹⁰See also recent analyses of these irregular conformal blocks in [18–20].

Let us describe this construction in more detail. We denote by $V_\alpha(z) =: e^{2\alpha\varphi(z)}:$ the Virasoro chiral vertex operator of “momentum” $\alpha \in \mathbb{C}$, central charge

$$c = 1 + 6Q^2, \quad Q = b + b^{-1},$$

and conformal weight

$$\Delta_\alpha = \alpha(Q - \alpha).$$

The standard degenerate primaries occur at

$$\alpha_{r,s} = \frac{1-r}{2}b + \frac{1-s}{2}b^{-1}, \quad r, s \in \mathbb{Z}_{>0},$$

with

$$V_{r,s}(z) = : e^{2\alpha_{r,s}\varphi(z)}:, \quad \Delta_{r,s} = \alpha_{r,s}(Q - \alpha_{r,s}) = \Delta_0 - \frac{(rb + sb^{-1})^2}{4},$$

where

$$\Delta_0 = \frac{Q^2}{4} = \frac{c-1}{24}.$$

The Gaiotto–Witten conformal block is defined as the chiral correlator

$$\int_{\Gamma} \left\langle I_{\alpha,\gamma}(\infty) \prod_{i=1}^L V_{-\frac{k_i}{2b}}(z_i) \prod_{\nu=1}^M V_{\frac{1}{b}}(E_\nu) \right\rangle dE_1 \dots dE_M,$$

where the degenerate primaries

$$V_{-\frac{k_i}{2b}}(z_i) \equiv V_{1,k_i+1}(z_i), \quad k_i \in \mathbb{N}_{>0},$$

are inserted at positions z_i , and the operators $V_{\frac{1}{b}}(E_\nu)$ are integrated over appropriate contours. Crucially, the chiral correlator also includes a single rank-one irregular vertex operator

$$I_{\alpha,\gamma}(z) \equiv : e^{2\alpha\varphi(z)} e^{\gamma\partial\varphi(z)}:$$

inserted at $z = \infty$.¹¹ Taken together, these ingredients define the irregular, degenerate conformal block, which can be represented as follows [19]:

$$\mathcal{F}_\Gamma(\mathbf{z}, \mathbf{k}) = \int_{\Gamma} \exp \left[-\frac{1}{b^2} \mathcal{W}^{\text{GW}}(\mathbf{z}, \mathbf{E}, \mathbf{k}) \right] dE_1 \dots dE_M, \quad (3.29)$$

where

$$\begin{aligned} \mathcal{W}^{\text{GW}}(\mathbf{z}, \mathbf{E}, \mathbf{k}) &= \frac{1}{2} \sum_{i < j} k_i k_j \log(z_i - z_j) + 2 \sum_{\nu < \mu} \log(E_\nu - E_\mu) \\ &\quad - \sum_i \sum_\nu k_i \log(E_\nu - z_i) - \Lambda \left(-\frac{1}{2} \sum_i k_i z_i + \sum_\nu E_\nu \right). \end{aligned} \quad (3.30)$$

¹¹Cf. appendix D.

In (3.29), Γ may be chosen to be any contour obtained by deforming the integration paths of the screening charges so as to ensure convergence of the integral. In (3.30), Λ represents a constant that is directly proportional to the eigenvalue of the rank-one irregular state when acted upon by the Virasoro generator L_1 .

Let us note that when we specialize to $\mathbf{k} = \{k_i = 1\}_{i=1}^L$ the Gaiotto–Witten YY function $\mathbb{W}(\mathbf{z}, \mathbf{E}) \equiv \mathcal{W}^{\text{GW}}(\{z_i\}, \{E_\nu\}, \{1\})$ coincides with the Richardson YY function $\mathcal{W}^{\text{R}}(\mathbf{z}, \mathbf{E})$ defined in (3.24). More precisely, one finds $\mathcal{W}^{\text{R}}(\mathbf{z}, \mathbf{E}) = -2\mathbb{W}(\mathbf{z}, \mathbf{E}) + 2\pi i LM$, provided that the identification $\frac{1}{g} = \Lambda$ is made between the Richardson coupling g and the “irregularity” parameter Λ . Therefore, the extremal value $\mathbb{W}_{\text{crit}}(\mathbf{z}, \mathbf{E}^c)$ encodes the conserved charges of the reduced BCS model. Indeed, since $\partial_{E_\nu} \mathcal{W}^{\text{R}} = -2\partial_{E_\nu} \mathbb{W}$ and $\partial_{z_i} \mathcal{W}^{\text{R}} = -2\partial_{z_i} \mathbb{W}$, it follows from (3.23) that

$$\lambda_i = -\frac{1}{\Lambda} \frac{\partial \mathbb{W}_{\text{crit}}(\mathbf{z}, \mathbf{E}^c)}{\partial z_i} \bigg|_{z_i=2\epsilon_i}.$$

The key question is whether this correspondence offers genuinely new insights. As noted above, expressing the critical Yang–Yang function $\mathcal{W}_{\text{crit}}^{\text{R}}$ in terms of irregular Gaiotto–Witten blocks immediately grants access to the full toolkit of 2D CFT. In particular, these blocks are degenerate—hence they satisfy BPZ [21] differential equations arising from the decoupling of null states. By taking the classical (large- c , $b \rightarrow 0$) limit of those BPZ equations and performing a saddle-point analysis, one recovers precisely the equations governing $\mathcal{W}_{\text{crit}}^{\text{R}}$, in direct analogy to how BPZ equations control classical conformal blocks. This observation opens the door to analytic methods for studying $\mathcal{W}_{\text{crit}}^{\text{R}}$.

4 Eigenvalue–based reformulation

4.1 Eigenvalue–based method

This section begins by rewriting the Richardson equations (3.15) using a new notation and a different indexing convention:

$$\frac{1}{g} - \sum_{\alpha=1}^L \frac{1}{\epsilon_\alpha - \lambda_j} + \sum_{\substack{k=1 \\ k \neq j}}^M \frac{2}{\lambda_k - \lambda_j} = 0, \quad \forall j = 1, \dots, M. \quad (4.1)$$

This reformulation aligns with the conventions widely adopted in the literature, particularly in the work of Faribault *et al.* [12], which serves as a primary reference throughout this section. The set of Bethe roots (*rapidities*), denoted in the previous section as $\{E_\nu\}$, is here denoted by $\{\lambda_j\}$. In addition, in equation (4.1) we performed a change of variable $2\epsilon \mapsto \epsilon$: originally 2ϵ represented the pair energy (with ϵ the single electron energy in the non-interacting limit), whereas now ϵ denotes the total energy of the Cooper pair.

Directly solving equations (4.1) with standard numerical algorithms for nonlinear systems is highly challenging due to the presence of singularities that occur when the rapidities

λ_j approach ϵ_α . To overcome this difficulty, we employ an alternative approach in which such singularities are avoided. As already mentioned, this section is based on the work [12], and it outlines techniques for solving the Richardson equations (4.1) using the so-called *eigenvalue-based method*.¹²

First, let us consider a polynomial of degree M in the form

$$P(z) = \prod_{j=1}^M (z - \lambda_j), \quad (4.2)$$

where z is a complex variable. The set $\{\lambda_j\}$ of roots of this polynomial corresponds to the set of rapidities, which are the solutions of the Richardson equations.

The derivative of $P(z)$ with respect to z is given by

$$P'(z) = \sum_{j=1}^M \left[\prod_{\substack{k=1 \\ k \neq j}}^M (z - \lambda_k) \right]. \quad (4.3)$$

We now define a function $\Lambda(z)$ as

$$\Lambda(z) = \frac{P'(z)}{P(z)} = \sum_{j=1}^M \frac{1}{z - \lambda_j}. \quad (4.4)$$

Its derivative is then given by

$$\Lambda'(z) = - \sum_{j=1}^M \frac{1}{(z - \lambda_j)^2}. \quad (4.5)$$

Clearly, $\Lambda(z)$ satisfies a Riccati-type differential equation [12]:

$$\frac{d\Lambda(z)}{dz} + \Lambda^2(z) = - \sum_{j=1}^M \frac{1}{(z - \lambda_j)^2} + \sum_{j,k=1}^M \frac{1}{(z - \lambda_j)(z - \lambda_k)}. \quad (4.6)$$

It can also be shown that if the set $\{\lambda_j\}$ satisfies the Bethe equations, then the following identity holds [12]:

$$\Lambda'(z) + \Lambda^2(z) - \sum_{\alpha=1}^M \frac{2F(\lambda_\alpha)}{(z - \lambda_\alpha)} = 0. \quad (4.7)$$

In our case, the function $F(\lambda_\alpha)$ will be given by

$$F(\lambda_\alpha) = - \sum_{i=1}^L \frac{A_i}{(\epsilon_i - \lambda_\alpha)} + \frac{B}{2g} \lambda_\alpha + \frac{C}{2g}. \quad (4.8)$$

The physical interpretation of the parameters ϵ_j and g is model-dependent. In the case of the Richardson equations, the set $\{\epsilon_j\}$ corresponds to the single particle energy levels, while g represents the coupling constant.

¹²See also [22].

Substituting this form of $F(\lambda_\alpha)$ into equation (4.7) yields:

$$\Lambda'(z) + \Lambda^2(z) - \sum_{\alpha=1}^M \frac{2}{(z - \lambda_\alpha)} \left[- \sum_{i=1}^L \frac{A_i}{(\epsilon_i - \lambda_\alpha)} + \frac{B}{2g} \lambda_\alpha + \frac{C}{2g} \right] = 0. \quad (4.9)$$

In the limit $z \rightarrow \epsilon_j$ we thus get

$$\begin{aligned} 0 &= \Lambda'(\epsilon_j) + \Lambda^2(\epsilon_j) + \sum_{\alpha=1}^M \sum_{i=1}^L \frac{2A_i}{(\epsilon_j - \lambda_\alpha)(\epsilon_i - \lambda_\alpha)} - \frac{B}{g} \sum_{\alpha=1}^M \frac{\lambda_\alpha}{(\epsilon_j - \lambda_\alpha)} \\ &\quad - \frac{C}{g} \sum_{\alpha=1}^M \frac{1}{(\epsilon_j - \lambda_\alpha)} \\ &= \Lambda'(\epsilon_j) + \Lambda^2(\epsilon_j) + \sum_{\alpha=1}^M \left[\sum_{i \neq j}^L \frac{2A_i}{(\epsilon_i - \lambda_\alpha)(\epsilon_j - \lambda_\alpha)} + \sum_{i=1}^L \frac{2A_i \delta_{ij}}{(\epsilon_i - \lambda_\alpha)(\epsilon_j - \lambda_\alpha)} \right] \\ &\quad - \sum_{\alpha=1}^M \frac{B\lambda_\alpha + C}{g(\epsilon_j - \lambda_\alpha)} \\ &= \Lambda'(\epsilon_j) + \Lambda^2(\epsilon_j) + \sum_{\alpha=1}^M \sum_{i \neq j}^L \frac{\epsilon_i - \epsilon_j}{\epsilon_i - \epsilon_j} \frac{2A_i}{(\epsilon_i - \lambda_\alpha)(\epsilon_j - \lambda_\alpha)} \\ &\quad + \sum_{\alpha=1}^M \frac{2A_j}{(\epsilon_j - \lambda_\alpha)(\epsilon_j - \lambda_\alpha)} - \sum_{\alpha=1}^M \frac{B\lambda_\alpha + B\epsilon_j - B\epsilon_j + C}{g(\epsilon_j - \lambda_\alpha)} \\ &= \Lambda'(\epsilon_j) + \Lambda^2(\epsilon_j) + \sum_{i \neq j}^L \frac{2A_i}{\epsilon_i - \epsilon_j} \sum_{\alpha=1}^M \frac{\epsilon_i - \lambda_\alpha - \epsilon_j + \lambda_\alpha}{(\epsilon_i - \lambda_\alpha)(\epsilon_j - \lambda_\alpha)} \\ &\quad + 2A_j \sum_{\alpha=1}^M \frac{1}{(\epsilon_j - \lambda_\alpha)^2} + \sum_{\alpha=1}^M \left[\frac{B(\epsilon_j - \lambda_\alpha)}{g(\epsilon_j - \lambda_\alpha)} - \frac{B\epsilon_j + C}{g(\epsilon_j - \lambda_\alpha)} \right] \\ &= \Lambda'(\epsilon_j) + \Lambda^2(\epsilon_j) + \sum_{i \neq j}^L \frac{2A_i}{\epsilon_i - \epsilon_j} \sum_{\alpha=1}^M \left[\frac{\epsilon_i - \lambda_\alpha}{(\epsilon_i - \lambda_\alpha)(\epsilon_j - \lambda_\alpha)} - \frac{\epsilon_j - \lambda_\alpha}{(\epsilon_i - \lambda_\alpha)(\epsilon_j - \lambda_\alpha)} \right] \\ &\quad + 2A_j [-\Lambda'(\epsilon_j)] + \sum_{\alpha=1}^M \frac{B}{g} - \frac{B\epsilon_j + C}{g} \sum_{\alpha=1}^M \frac{1}{\epsilon_j - \lambda_\alpha} \\ &= \Lambda'(\epsilon_j) + \Lambda^2(\epsilon_j) + \sum_{i \neq j}^L \frac{2A_i}{\epsilon_i - \epsilon_j} \sum_{\alpha=1}^M \left[\frac{1}{\epsilon_j - \lambda_\alpha} - \frac{1}{\epsilon_i - \lambda_\alpha} \right] \\ &\quad - 2A_j \Lambda'(\epsilon_j) + \frac{B}{g} M - \frac{B\epsilon_j + C}{g} \Lambda(\epsilon_j) \\ &= (1 - 2A_j) \Lambda'(\epsilon_j) + \Lambda^2(\epsilon_j) + \sum_{i \neq j}^L \frac{2A_i [\Lambda(\epsilon_j) - \Lambda(\epsilon_i)]}{\epsilon_i - \epsilon_j} + \frac{B}{g} M - \frac{B\epsilon_j + C}{g} \Lambda(\epsilon_j). \quad (4.10) \end{aligned}$$

In the pseudospin models we assume that $A_i = |s_i| \Omega_i$, where $|s_i|$ is the norm of the local spin degree of freedom, and Ω_i is an integer related to the degeneracy.

4.2 Application to Richardson's equations

Let us now examine the form of $F(\lambda_\alpha)$ and the Richardson equations (4.1) cast in the form

$$-\sum_{\substack{k=1 \\ k \neq j}}^M \frac{1}{\lambda_k - \lambda_j} = -\sum_{\alpha=1}^L \frac{1}{2(\epsilon_\alpha - \lambda_j)} + \frac{1}{2g}. \quad (4.11)$$

We observe that the right-hand side of equation (4.11) takes the same form as $F(\lambda_j)$ if we choose $A_i = \frac{1}{2}$, $B = 0$, and $C = 1$. Substituting these values into the general solution (4.10) yields:

$$\Lambda^2(\epsilon_j) + \sum_{i \neq j}^L \frac{\Lambda(\epsilon_j) - \Lambda(\epsilon_i)}{\epsilon_i - \epsilon_j} + \frac{1}{g} \Lambda(\epsilon_j) = 0, \quad j = 1, \dots, M, \quad (4.12)$$

which is a set of M quadratic equations for $\Lambda(\epsilon_j)$. For simplicity let us multiply (4.12) by g^2 , and substitute $\Lambda_j = g\Lambda(\epsilon_j)$. Then, one gets

$$\Lambda_j^2 + g \sum_{i \neq j}^L \frac{\Lambda_j - \Lambda_i}{\epsilon_i - \epsilon_j} + \Lambda_j = 0, \quad j = 1, \dots, M. \quad (4.13)$$

This set of equations can be solved numerically using a variety of methods, one of which is the Newton–Raphson method.

For the boundary conditions at $g = 0$ we take

$$\Lambda_j = \begin{cases} 1 & \text{if } \epsilon_j \text{ is occupied,} \\ 0 & \text{if } \epsilon_j \text{ is not occupied.} \end{cases} \quad (4.14)$$

Solving (4.13) up to desired precision gives us a set of M values of Λ_j . After dividing by g , we get desired values of $\Lambda(\epsilon_j)$. We can use these values to find the coefficients of polynomials $P(z)$. If we write $P(z)$ and $P'(z)$ in the form

$$P(z) = \sum_{m=0}^M P_{M-m} z^m, \quad P'(z) = \sum_{m=0}^M m P_{M-m} z^{m-1}, \quad (4.15)$$

we have

$$\Lambda(z) = \frac{\sum_{m=0}^M m P_{M-m} z^{m-1}}{\sum_{m=0}^M P_{M-m} z^m} \Rightarrow \Lambda(\epsilon_j) = \frac{\sum_{m=0}^M m P_{M-m} \epsilon_j^{m-1}}{\sum_{m=0}^M P_{M-m} \epsilon_j^m}, \quad (4.16)$$

with $P_0 = 1$. It is worth noting that the index $M - m$ does not refer to the power of z , but rather to the order of the product over the roots λ_j . Given L known values of $\Lambda(\epsilon_j)$, the problem can be reduced to a linear one. We obtain:

$$\sum_{m=0}^M P_{M-m} \epsilon_j^m \Lambda(\epsilon_j) = \sum_{m=0}^M m P_{M-m} \epsilon_j^{m-1} \Rightarrow$$

$$\begin{aligned}
\sum_{m=0}^{M-1} P_{M-m} \epsilon_j^m \Lambda(\epsilon_j) + P_{M-M} \epsilon_j^M \Lambda(\epsilon_j) &= \sum_{m=0}^{M-1} m P_{M-m} \epsilon_j^{m-1} + M P_{M-M} \epsilon_j^{M-1} \Rightarrow \\
\epsilon_j^M \Lambda(\epsilon_j) - M \epsilon_j^{M-1} &= \sum_{m=0}^{M-1} \left[m \epsilon_j^{m-1} P_{M-m} - \epsilon_j^m \Lambda(\epsilon_j) P_{M-m} \right] \Rightarrow \\
\sum_{m=0}^{m-1} \left[m \epsilon_j^{m-1} - \epsilon_j^m \Lambda(\epsilon_j) \right] P_{M-m} &= \epsilon_j^M \Lambda(\epsilon_j) - M \epsilon_j^{M-1}, \tag{4.17}
\end{aligned}$$

which is a set of L linear equations for $M - 1$ coefficients of $P(z)$.

In the case where $M < L$ and the resulting system of equations is directly solvable, one can construct the polynomial $P(z)$ and determine its roots using the Laguerre method with polynomial deflation. This approach is particularly effective because the Laguerre method is guaranteed to converge to at least one (possibly complex) root. Polynomial deflation subsequently allows us to reduce the degree of the polynomial by factoring out the discovered root, thereby simplifying the root-finding problem. Repeating this procedure enables the systematic determination of all roots of the polynomial.

To determine the dependence of the rapidities $\{\lambda_j\}$ on the coupling constant g , we begin with the initial values of Λ_j given by equation (4.14). The first set of rapidities is computed for a small, non-zero value of g . In subsequent iterations, g is incrementally increased by a small factor, and the previously obtained values of Λ_j are used as initial conditions for the next step. This iterative procedure allows for a controlled and continuous tracking of the evolution of the rapidities as a function of the coupling strength.

In the case where $M > L$, the system of equations given in (4.17) becomes underdetermined and cannot be solved directly. This corresponds to a degenerate scenario. To address this issue, the energy levels are extended into the complex domain such that each Cooper pair occupying a degenerate energy level ϵ_j is assigned to a distinct complex energy level ε_j , defined by

$$\varepsilon_j = \epsilon_j + ik, \quad k = -\frac{d_j - 1}{2}, -\frac{d_j - 1}{2} + 1, \dots, \frac{d_j - 1}{2} - 1, \frac{d_j - 1}{2}, \tag{4.18}$$

where d_j denotes the degeneracy of the energy level ϵ_j in the $g = 0$ limit. For example, if the level ϵ_j is occupied by three Cooper pairs, then $d_j = 3$, and the corresponding complex levels are $\varepsilon_j = \epsilon_j - i$, ϵ_j , and $\epsilon_j + i$. This extension into the complex plane guarantees that the number of distinct ε_j matches the number of Cooper pairs, ensuring solvability of the system. Moreover, the symmetric distribution of the complex shifts about the real axis preserves the reality of the total energy.

5 Numerical implementation

In this section, we present the details of the numerical implementation used to solve the Richardson equations. The primary goal of the program is to efficiently compute the

rapidities for varying values of the coupling constant g , including both non-degenerate and degenerate cases. The implementation combines symbolic preprocessing with robust numerical algorithms, such as Newton–Raphson iteration and the Laguerre method with polynomial deflation, to ensure stability and convergence.

The structure of the code was designed to be modular and flexible, allowing for straightforward extension to related models. This section outlines the overall architecture of the program, the key numerical methods employed, and practical considerations such as initialization strategies, handling of complex roots, and performance optimization.

We begin by characterizing the numerical methods mentioned above.

5.1 LU decomposition

Let us consider a system of N linear equations in matrix form:

$$\mathbf{A} \mathbf{x} = \mathbf{b}, \quad (5.1)$$

where \mathbf{A} is an $N \times N$ matrix, \mathbf{b} is a given N -element column vector, and \mathbf{x} is the unknown N -element column vector that satisfies this equation. Suppose that \mathbf{A} admits an LU factorization,

$$\mathbf{A} = \mathbf{L} \mathbf{U}, \quad (5.2)$$

where \mathbf{L} is a lower triangular matrix with entries α_{ij} ($\alpha_{ij} = 0$ for $j > i$), and \mathbf{U} is an upper triangular matrix with entries β_{ij} ($\beta_{ij} = 0$ for $j < i$). Then (5.1) becomes

$$\mathbf{L} \mathbf{U} \mathbf{x} = \mathbf{b}. \quad (5.3)$$

If we set $\mathbf{U} \mathbf{x} = \mathbf{y}$, then

$$\mathbf{L} \mathbf{y} = \mathbf{b}. \quad (5.4)$$

Since \mathbf{L} is lower triangular, we solve (5.4) by forward substitution. The first component is

$$y_0 = \frac{b_0}{\alpha_{00}}, \quad (5.5)$$

and the remaining components follow iteratively as

$$y_i = \frac{1}{\alpha_{ii}} \left[b_i - \sum_{j=0}^{i-1} \alpha_{ij} y_j \right], \quad i = 1, 2, \dots, N-1. \quad (5.6)$$

Having obtained \mathbf{y} , we solve $\mathbf{U} \mathbf{x} = \mathbf{y}$ by back substitution:

$$x_{N-1} = \frac{y_{N-1}}{\beta_{N-1, N-1}}, \quad (5.7)$$

$$x_i = \frac{1}{\beta_{ii}} \left[y_i - \sum_{j=i+1}^{N-1} \beta_{ij} x_j \right], \quad i = N-2, N-3, \dots, 0. \quad (5.8)$$

5.2 Newton–Raphson method

Consider a system of N nonlinear equations,

$$F_i(x_0, x_1, \dots, x_{N-1}) = 0, \quad i = 0, 1, \dots, N-1. \quad (5.9)$$

We write the vector of unknowns as \mathbf{x} and the vector of functions as $\mathbf{F}(\mathbf{x})$. In the neighborhood of \mathbf{x} , a first order Taylor expansion gives

$$\mathbf{F}(\mathbf{x} + \delta\mathbf{x}) = \mathbf{F}(\mathbf{x}) + \sum_{j=0}^{N-1} \frac{\partial F_i}{\partial x_j} \delta x_j + \mathcal{O}(\|\delta\mathbf{x}\|^2). \quad (5.10)$$

The partial derivatives define the Jacobian matrix,

$$J_{ij} = \frac{\partial F_i}{\partial x_j}, \quad (5.11)$$

so that

$$\mathbf{F}(\mathbf{x} + \delta\mathbf{x}) = \mathbf{F}(\mathbf{x}) + \mathbf{J} \delta\mathbf{x} + \mathcal{O}(\|\delta\mathbf{x}\|^2). \quad (5.12)$$

Setting $\mathbf{F}(\mathbf{x} + \delta\mathbf{x}) = \mathbf{0}$ and neglecting higher order terms yields the linear system

$$\mathbf{J} \delta\mathbf{x} = -\mathbf{F}(\mathbf{x}), \quad (5.13)$$

which can be solved for $\delta\mathbf{x}$ by LU decomposition. Updating the solution,

$$\mathbf{x}_{\text{new}} = \mathbf{x}_{\text{init}} + \delta\mathbf{x}, \quad (5.14)$$

and iterating this process yields successive approximations until the desired accuracy is achieved.

5.3 Laguerre method for root finding

Consider a polynomial of degree n defined by

$$P_n(x) = (x - x_0)(x - x_1) \cdots (x - x_{n-1}), \quad (5.15)$$

$$\log|P_n(x)| = \log|x - x_0| + \log|x - x_1| + \cdots + \log|x - x_{n-1}|. \quad (5.16)$$

In the Laguerre method we introduce the functions

$$G(x) = \frac{d}{dx} \log|P_n(x)| = \sum_{i=0}^{n-1} \frac{1}{x - x_i} = \frac{P'_n(x)}{P_n(x)}, \quad (5.17)$$

$$H(x) = -\frac{d^2}{dx^2} \log|P_n(x)| = \sum_{i=0}^{n-1} \frac{1}{(x - x_i)^2} = \left[\frac{P'_n(x)}{P_n(x)} \right]^2 - \frac{P''_n(x)}{P_n(x)}. \quad (5.18)$$

Assume that one root, x_0 , lies at distance a from the current estimate x , while all other roots lie at the same distance b . That is,

$$x - x_0 = a, \quad x - x_i = b \quad (i \neq 0).$$

Substituting these into the definitions of $G(x)$ and $H(x)$ gives

$$G(x) = \frac{1}{a} + \frac{n-1}{b}, \quad (5.19)$$

$$H(x) = \frac{1}{a^2} + \frac{n-1}{b^2}. \quad (5.20)$$

Solving for a yields

$$a = \frac{n}{G(x) \pm \sqrt{(n-1)[nH(x) - G^2(x)]}}, \quad (5.21)$$

where the sign is chosen to minimize $|a|$. Starting from an initial estimate x , one computes a and updates

$$x \leftarrow x - a,$$

iterating until $|a|$ is below a chosen tolerance, at which point $x \approx x_0$.

Polynomial deflation consists of factoring

$$P_n(x) = (x - r) Q_{n-1}(x),$$

where r is a found root and $Q_{n-1}(x)$ is a polynomial of degree $n-1$. One then applies the Laguerre method to $Q_{n-1}(x)$ to locate another root of $P_n(x)$, and repeats until all n roots are determined.

5.4 Code structure

The purpose of the program is to compute the energy of Cooper pairs in the Richardson model using an eigenvalue-based method. The system structure (number of Cooper pairs, energy levels, and degeneracies) is read from input `.txt` files. The source code and a guide for preparing the input files are available on GitHub:

[<https://github.com/GrzegorzBiskowski/Richardson-solver>].

After the computation, the program saves the energy as a function of the coupling constant g in both `.txt` and `.csv` formats.

General workflow. After loading the data, the program initializes the starting value of g and begins the first iteration of a `do-while` loop. It first solves a system of nonlinear equations using the Newton–Raphson method, where the associated linear system is handled via LU decomposition. The resulting Λ values are then used to build another linear system for the coefficients of the polynomials $P(z)$.

Ultimately, the Cooper pair energies are computed using the Laguerre method with polynomial deflation and written to a file. Each iteration concludes by incrementing g by a small step. The loop continues until a target value of g is reached. In this study, the final value used was $g = 1.5$.

Code architecture. The program consists of three main files: `main.cpp`, `solver.cpp`, and `solver.h`. The file `solver.h` contains class declarations, while `solver.cpp` defines the corresponding methods.

Three main classes were developed:

- `cSqMatrix`
- `cEquations`
- `cPolynomials`

`cSqMatrix` stores square matrices and is responsible for solving linear systems. The right-hand side vector is passed via the constructor, which immediately invokes LU decomposition. The solution then replaces the original input vector.

`cEquations` solves the nonlinear system for Λ values. It includes the method `function_i`, which returns the left-hand side of the equation for a given index i and vector of values, as well as `newton_raphson`, which updates the *initial guess* with the solution obtained via the Newton–Raphson method.

`cPolynomials` takes the energy vector of elements E_j (from the previous iteration, or equal to ϵ_j in the first iteration), the value of g , and the previously computed Λ values. It builds a matrix of type `cSqMatrix` for the polynomial coefficients, which are then calculated using LU decomposition. The Cooper pair energies are obtained by finding the roots using the Laguerre method, implemented in the `root_finder` function. This class also provides helper methods: `value`, `first_der`, and `second_der`, which compute the polynomial value, first derivative, and second derivative, respectively, for a given argument (the current guess in the Laguerre method).

Libraries and tools. The following C++ standard libraries are used:

- `iostream`
- `fstream`
- `iomanip`
- `cmath`
- `complex`

The first three handle file I/O and console output. In particular, `cout` is used to print the current g value to the console for monitoring purposes. The `complex` library is essential for the Laguerre method, which must compute both real and complex roots of $P(z)$. Consequently, all program variables are declared as `std::complex<double>`, including the ϵ vector. This also reflects the convention used for energy splitting in the complex plane given by (4.18).

Development environment and stability. The code was written using the Code::Blocks 20.03 IDE and compiled using `g++`. The program performs with high numerical stability and accuracy for systems with up to 20 Cooper pairs. For larger systems, small discontinuities may occasionally appear in the Λ solutions, which can influence the precision of the resulting energies. However, this opens the door to future improvements, such as fine-tuning numerical parameters or incorporating adaptive stabilization techniques to extend the solver’s robustness to even larger systems.

It should be noted that all algorithms were deliberately implemented in their most basic form, without incorporating advanced numerical stabilization techniques. This simplicity constitutes a practical advantage, as it enables both straightforward use and further development of the code without requiring specialized programming or numerical analysis expertise.

6 Example calculations and applications

6.1 Non-degenerate solutions

The methods described in the previous sections were used to compute the energy spectrum of the Cooper pairs, E_J , as a function of the coupling constant g for various models.¹³

We first consider the one-dimensional quantum harmonic oscillator with $L = 12$ levels,

$$\epsilon_j = j + \frac{1}{2}, \quad j = 0, 1, \dots, 11,$$

occupied by $M = 6$ Cooper pairs filling the lowest available levels. Figures 2 and 3 display

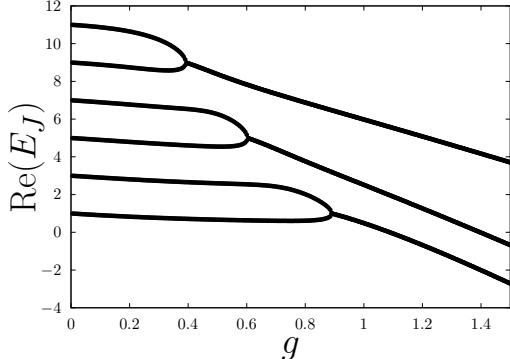


Figure 2. Real Cooper pair energies for the picket-fence model with $L = 12$ levels and $M = 6$ pairs.

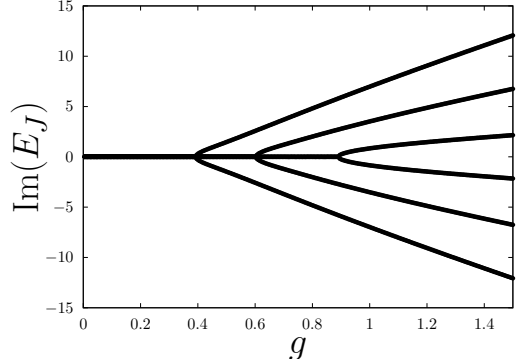


Figure 3. Imaginary Cooper pair energies for the picket-fence model with $L = 12$ levels and $M = 6$ pairs.

the real and imaginary parts of the Cooper pair energies, respectively. The real parts

¹³In this subsection, all energies are given per single electron; consequently, at $g = 0$ each Cooper pair has twice the listed energy.

begin to coalesce at different values of g , depending on the initial energy levels; these characteristic arcs also appear in subsequent examples.

According to the Richardson equations, a singularity would occur when $E_{J_\nu} = E_{J_\mu}$ for $\mu \neq \nu$. However, by allowing the energies to extend into the complex plane, the imaginary parts branch out precisely at the points where two real parts merge. Figure 3 shows that this branching is symmetric, thereby preserving the reality of the total energy.

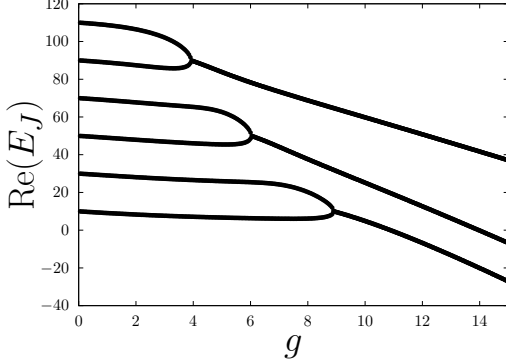


Figure 4. Real Cooper pair energies for the picket-fence model with $L = 12$ levels and $M = 6$ pairs.

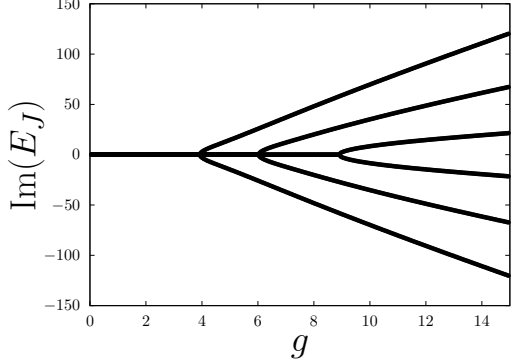


Figure 5. Imaginary Cooper pair energies for the picket-fence model with $L = 12$ levels and $M = 6$ pairs.

In the next example, the single particle energies are given by

$$\epsilon_j = 10 \times \left(j + \frac{1}{2}\right), \quad j = 0, 1, \dots, 11,$$

and the coupling constant g is scaled by a factor of 10 in Figures 4 and 5. Despite multiplying both g and ϵ_j by 10, the resulting spectra are identical. Figures 6 and 7 display

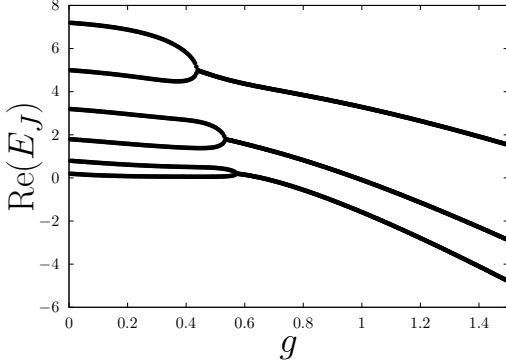


Figure 6. Real Cooper pair energies for the 1D infinite potential well with $L = 12$ levels and $M = 6$ pairs.

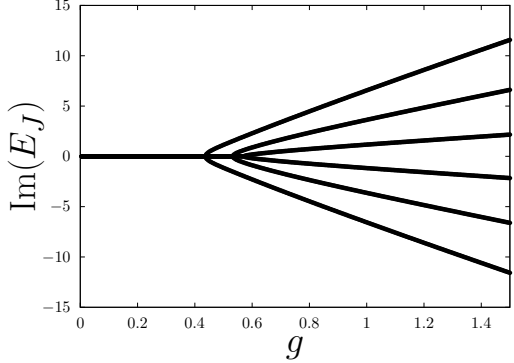


Figure 7. Imaginary Cooper pair energies for the 1D infinite potential well with $L = 12$ levels and $M = 6$ pairs.

the real and imaginary parts of the Cooper pair spectrum, respectively, for $M = 6$ pairs

occupying $L = 12$ levels with single particle energies $\epsilon_j \propto j^2$, corresponding to the infinite potential well model.

Notice that the lowest lying levels merge at smaller values of g , reflecting the reduced initial energy spacing between these levels.

In the next example, we choose single particle energies to follow a hydrogen-like spectrum,

$$\epsilon_j \propto -\frac{1}{j^2}, \quad j = 1, 2, \dots,$$

and the resulting real and imaginary parts of the Cooper pair energies are shown in Figures 8 and 9, respectively. Figures 8 and 9 display the energies of $M = 6$ Cooper pairs

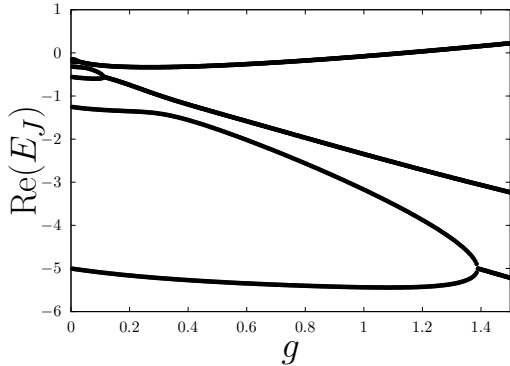


Figure 8. Real Cooper pair energies for the $\epsilon_j \propto -j^{-2}$ model with $L = 6$ levels and $M = 6$ pairs.

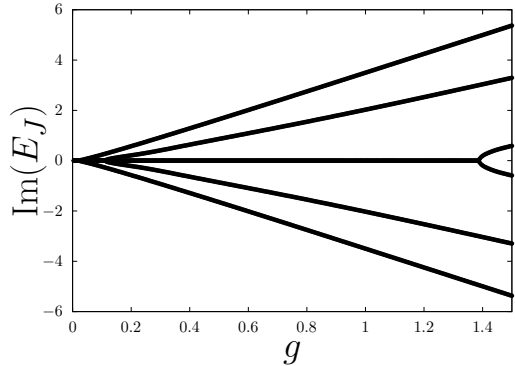


Figure 9. Imaginary Cooper pair energies for the $\epsilon_j \propto -j^{-2}$ model with $L = 6$ levels and $M = 6$ pairs.

distributed among the $L = 6$ highest single particle levels. The spacing between the two highest levels is extremely small compared to that between the two lowest levels, so the former merge almost immediately as g increases, whereas the latter coalesce only around $g \approx 1.4$.

6.2 Degenerate solutions

Similar calculations were carried out for the degenerate case using the two-dimensional quantum harmonic oscillator. Here the single particle energies scale as

$$\epsilon_j = 2j, \quad j = 0, 1, 2, \dots,$$

with degeneracies

$$D_j = j.$$

Figures 10 and 11 show the solutions of the Richardson equations for $M = 6$ Cooper pairs distributed over $L = 4$ levels, where the first three levels are fully occupied and the highest level is empty. Due to the method chosen for handling degeneracies, the imaginary parts of the energies do not start at zero when $g = 0$, as they do in the non-degenerate cases.

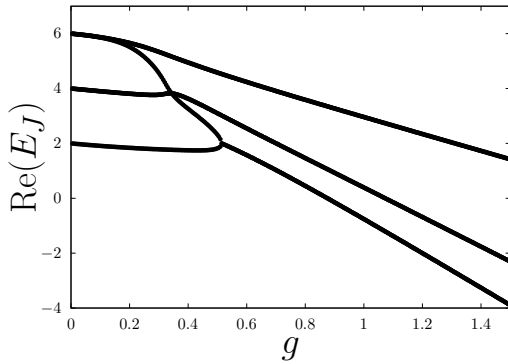


Figure 10. Real Cooper pair energies for the 2D harmonic oscillator with $L = 4$ levels and $M = 6$ pairs.

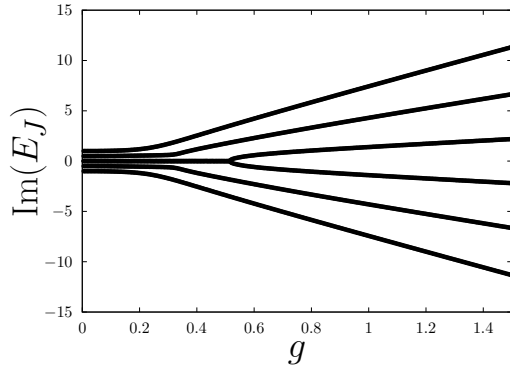


Figure 11. Imaginary pair energies for the 2D harmonic oscillator with $L = 4$ levels and $M = 6$ pairs.

Here, the initial energies are set according to equation (4.18), which modifies the initial values of $\text{Im}(E_J)$. Nevertheless, the branching behaviour of $\text{Im}(E_J)$ as g increases closely resembles that seen in the non-degenerate solutions.

For the real parts, we observe that the energies do not fully coalesce as they did in the one-dimensional harmonic oscillator. After the first merging at $g \approx 0.3$, one branch immediately re-splits: one sub-branch merges with the ground state energy, while the other remains separate.

We then solved the Richardson equations for the two-dimensional infinite square well, with $M = 6$ Cooper pairs occupying the lowest four of the $L = 5$ available levels. The resulting real and imaginary spectra are presented in Figures 12 and 13, respectively. This example was selected because the level degeneracies follow no simple pattern and the

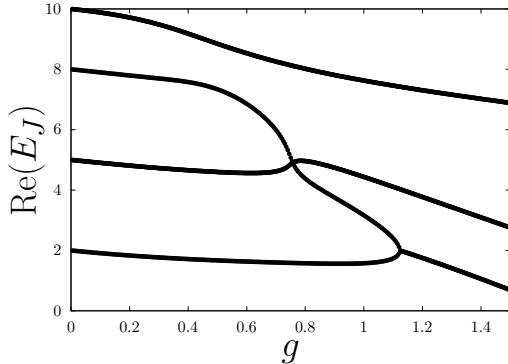


Figure 12. Real Cooper pair energies for the 2D infinite potential square well with $L = 5$ levels and $M = 6$ pairs.

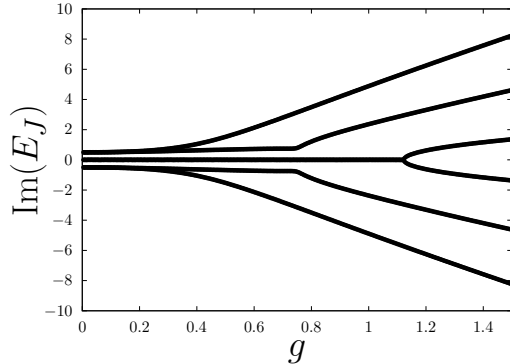


Figure 13. Imaginary Cooper pair energies for the 2D infinite potential square well with $L = 5$ levels and $M = 6$ pairs.

energies do not lie on an elementary series. Nevertheless, the behaviour closely resembles that of the two-dimensional quantum harmonic oscillator: pairs of solutions coalesce and

then immediately branch, with one branch subsequently merging into the lowest energy state. The imaginary part of the spectrum exhibits a pronounced cusp near $g \approx 0.8$, which arises from the initial imaginary separations of the levels; detailed numerical tests confirm that the magnitude of this initial separation does not affect the real spectrum.

It is also noteworthy that, in both the two-dimensional harmonic oscillator and the two-dimensional infinite square well, certain degenerate levels remain inert and do not participate in any merging or branching.

Finally, we consider a two-level model with $M = 16$ Cooper pairs equally distributed between the levels $\epsilon = \pm 1$. The resulting real and imaginary parts of the pair energies are shown in Figures 14 and 15, respectively. This model does not exhibit the characteristic

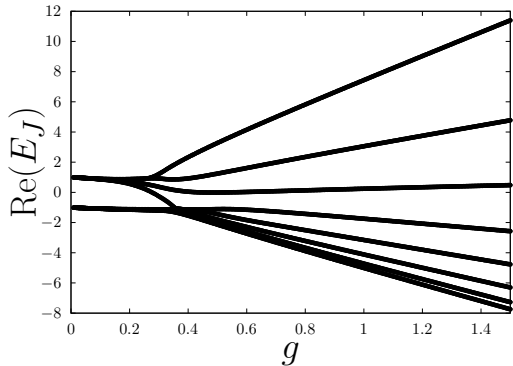


Figure 14. Real Cooper pair energies for the two-level model with $M = 16$ pairs.

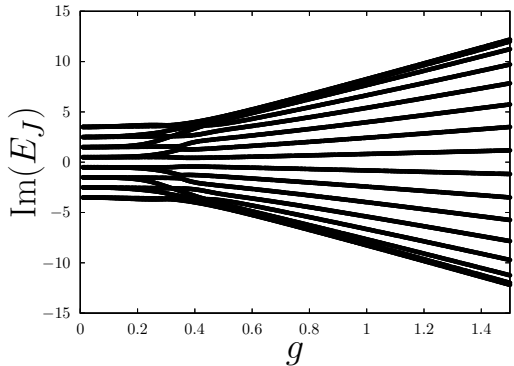


Figure 15. Imaginary Cooper pair energies for the two-level model with $M = 16$ pairs.

merging observed previously. Highly degenerate systems tend to favour branching of energy levels, whereas non-degenerate systems promote the merging of the closest levels (in terms of energy gap). Here, each level has degeneracy $D_J = 8$, so the energies branch out and approach a distribution resembling a down-shifted j^2 spectrum. Notably, at $g = 1.5$ the sixteen Cooper pair energies collapse into only eight distinct values, indicating that branching stops at pairs of levels rather than proceeding fully.

6.3 Thermal pairing

Thermodynamic effects can be incorporated into the Richardson model by statistically averaging exact many-body eigenenergies over a thermal ensemble. Since the total number of fermions N is fixed, the canonical ensemble is the natural framework: it preserves particle number while allowing the system's energy to fluctuate according to temperature.

A central observable in this context is the *temperature-dependent pairing energy*, defined as the thermal average energy difference between the interacting ($g \neq 0$) and non-interacting ($g = 0$) systems (cf. [23]):

$$E_p(g, T) = \langle E(g) \rangle - \langle E(g = 0) \rangle, \quad (6.1)$$

where the thermal average $\langle E \rangle$ is given by

$$\langle E \rangle = \frac{1}{Z} \sum_{\alpha} D_{\alpha} E_{\alpha} \exp\left(-\frac{E_{\alpha}}{kT}\right), \quad (6.2)$$

and the canonical partition function is

$$Z = \sum_{\alpha} D_{\alpha} \exp\left(-\frac{E_{\alpha}}{kT}\right). \quad (6.3)$$

Here, E_{α} are the exact eigenenergies of the system, D_{α} their degeneracies, and k is the Boltzmann constant.

The temperature dependence of the internal energy $\langle E \rangle$ further allows for direct computation of thermodynamic quantities. In particular, the *heat capacity* at fixed particle number is obtained via

$$C_V(T) = \frac{\partial \langle E \rangle}{\partial T} \Big|_{N,V}. \quad (6.4)$$

This framework enables finite-temperature studies of pairing phenomena in finite-size systems, without resorting to mean-field or grand canonical approximations. It also provides a concrete benchmark for testing extensions of the Bethe ansatz to thermodynamic regimes.

In the case of the two-level Richardson model, all Cooper pair eigenenergies (Bethe rapidities) and their associated degeneracies can be determined explicitly. For instance, Ciechan and Wysokiński [23] computed the complete spectrum for $M = 10$ pairs and used direct state summation to evaluate the specific heat and pairing energy as functions of T . Using our solver, we can readily reproduce these results and extend them to larger system sizes—namely, systems with more than two energy levels ($L > 2$) and over ten pairs ($M > 10$)—as well as to finer temperature grids. These results, among others, will be presented in a forthcoming paper.

6.4 Yang–Yang function and classical conformal blocks

As an example of the correspondence between the classical limit of conformal blocks and quantum integrable systems of the Richardson–Gaudin type, let us consider the Coulomb gas representation of a spherical Virasoro four-point block:

$$\begin{aligned} \mathcal{Z}(\cdot | \mathbf{z}_f) &= \left\langle : e^{\hat{\alpha}_1 \phi(0)} : : e^{\hat{\alpha}_2 \phi(x)} : : e^{\hat{\alpha}_3 \phi(1)} : : e^{\hat{\alpha}_4 \phi(\infty)} : \left[\int_0^x e^{b\phi(E)} dE \right]^{M_1} \left[\int_0^1 e^{b\phi(E)} dE \right]^{M_2} \right\rangle \\ &= x^{\frac{\alpha_1 \alpha_2}{2\beta}} (1-x)^{\frac{\alpha_2 \alpha_3}{2\beta}} \times \\ &\quad \times \prod_{\mu=1}^{M_1} \int_0^x dE_{\mu} \prod_{\mu=M_1+1}^{M_1+M_2} \int_0^1 dE_{\mu} \prod_{\mu < \nu} (E_{\nu} - E_{\mu})^{2\beta} \prod_{\mu} E_{\mu}^{\alpha_1} (E_{\mu} - x)^{\alpha_2} (E_{\mu} - 1)^{\alpha_3}, \end{aligned}$$

where $\mathbf{z}_f = (0, x, 1, \infty)$. It was not clear for a long time how to choose integration contours to get an integral representation of the four-point block consistent with historically first

BPZ power series representation [21]:

$$\mathcal{F}(\Delta_4, \dots, \Delta_1, \Delta, c | x) = x^{\Delta - \Delta_2 - \Delta_1} \left(1 + \sum_{n=1}^{\infty} x^n \mathcal{F}_n(\Delta_4, \dots, \Delta_1, \Delta, c) \right),$$

$$\mathcal{F}_n(\Delta_4, \dots, \Delta_1, \Delta, c) = \sum_{n=|I|=|J|} \langle \Delta_4 | V_{\Delta_3}(1) | \Delta_I^n \rangle \left[G_{c, \Delta}^{(n)} \right]^{IJ} \langle \Delta_J^n | V_{\Delta_2}(1) | \Delta_1 \rangle.$$

Here, $\left[G_{c, \Delta}^{(n)} \right]^{IJ}$ denotes the inverse of the Gram matrix

$$\left[G_{c, \Delta}^{(n)} \right]_{IJ} = \langle \Delta_I^n | \Delta_J^n \rangle,$$

where

$$| \Delta_I^n \rangle = L_{-I} | \Delta \rangle = L_{-i_k} \dots L_{-i_2} L_{-i_1} | \Delta \rangle$$

is the standard basis of the subspace

$$\mathcal{V}_{(n, \Delta)} \subset \bigoplus_{n=0}^{\infty} \mathcal{V}_{(n, \Delta)}$$

of the Verma module. Basis vectors are labeled by partitions $I = (i_k \geq \dots \geq i_1 \geq 1)$, whose total length is $|I| := i_1 + \dots + i_k = n$. The symbols $V_{\Delta_j}(z)$ denote Virasoro chiral vertex operators,

$$V_{\Delta_j}(z) = V(| \Delta_j \rangle | z) = V_{\Delta_k, \Delta_i}^{\Delta_j} (| \Delta_j \rangle | z) : \mathcal{V}_{\Delta_i} \longrightarrow \mathcal{V}_{\Delta_k}$$

that act between Verma modules and are defined by (i) commutation relations with Virasoro generators,

$$[L_n, V_{\Delta}(z)] = z^n \left(z \frac{d}{dz} + (n+1)\Delta \right) V_{\Delta}(z);$$

(ii) normalization $\langle \Delta_3 | V_{\Delta_2}(z) | \Delta_1 \rangle = z^{\Delta_3 - \Delta_2 - \Delta_1}$.

Mironov, Morozov and Shakirov showed that $\mathcal{Z}(\cdot | \mathbf{z}_f)$ precisely reproduces the BPZ four-point block expansion [24]. This result holds assuming that

$$\Delta_i = \frac{\alpha_i(\alpha_i + 2 - 2\beta)}{4\beta}, \quad i = 1, 2, 3,$$

$$\Delta_4 = \frac{(2\beta(M_1 + M_2) + \alpha_1 + \alpha_2 + \alpha_3)(2\beta(M_1 + M_2) + \alpha_1 + \alpha_2 + \alpha_3 + 2 - 2\beta)}{4\beta},$$

$$\Delta = \frac{(2\beta M_1 + \alpha_1 + \alpha_2)(2\beta M_1 + \alpha_1 + \alpha_2 + 2 - 2\beta)}{4\beta},$$

$$c = 1 - 6 \left(\sqrt{\beta} - \frac{1}{\sqrt{\beta}} \right)^2, \quad \beta = b^2, \quad \alpha_i = 2b\hat{\alpha}_i.$$

Thus, there are two ways to compute the $b \rightarrow \infty$ asymptotic of $\mathcal{Z}(\cdot | \mathbf{z}_f)$. On the one hand, it corresponds to the saddle-point approximation of the integral. On the other hand, it coincides with the classical (large- c) limit of the BPZ four-point conformal block,

$$\mathcal{F}(\Delta_i, \Delta, c | x) \xrightarrow{b \rightarrow \infty} \exp \left[b^2 f(\delta_i, \delta | x) \right],$$

where we define

$$\delta_i = \lim_{b \rightarrow \infty} \frac{\Delta_i}{b^2}, \quad \delta = \lim_{b \rightarrow \infty} \frac{\Delta}{b^2}.$$

Equivalently,

$$f(\delta_i, \delta | x) = \lim_{b \rightarrow \infty} \frac{1}{b^2} \log \mathcal{F}(\Delta_i, \Delta, c | x).$$

In particular, the small- x expansion of the classical block reads

$$f(\delta_i, \delta | x) = (\delta - \delta_1 - \delta_2) \log x + \frac{(\delta + \delta_2 - \delta_1)(\delta + \delta_3 - \delta_4)}{2\delta} x + \mathcal{O}(x^2).$$

We therefore arrive at the following proposition. Set

$$\begin{aligned} \delta_i &= \eta_i(\eta_i - 1), \quad i = 1, 2, 3, \\ \delta_4 &= (M_1 + M_2 + \eta_1 + \eta_2 + \eta_3)(M_1 + M_2 + \eta_1 + \eta_2 + \eta_3 - 1), \\ \delta &= (M_1 + \eta_1 + \eta_2)(M_1 + \eta_1 + \eta_2 - 1). \end{aligned} \tag{6.5}$$

If the classical conformal weights are chosen as in (6.5), then the four-point classical block on the sphere can be written in closed form as follows:

$$\begin{aligned} f(\delta_i, \delta | x) &= -\mathcal{W}_{\text{crit}}(\mathbf{z}_f, \mathbf{E}^c) - \left[S_{M_1}(2\eta_1, 2\eta_2) + S_{M_2}(2(\eta_1 + \eta_2 + M_1), 2\eta_3) \right] \\ &\quad + 2\eta_1\eta_2 \log x + 2\eta_2\eta_3 \log(1 - x), \end{aligned} \tag{6.6}$$

where the YY function is

$$\begin{aligned} \mathcal{W}(\mathbf{z}_f, \mathbf{E}) &= -2 \sum_{\mu < \nu} \log(E_\nu - E_\mu) \\ &\quad - \sum_{\mu=1}^{M_1+M_2} \left[2\eta_1 \log E_\mu + 2\eta_2 \log(E_\mu - x) + 2\eta_3 \log(E_\mu - 1) \right]. \end{aligned}$$

The function $S_n(a, b)$ is obtained from the saddle-point asymptotics of the Selberg integral (see [25]). The critical parameters $\mathbf{E}^c = \{E_1^c, \dots, E_M^c\}$, with $M = M_1 + M_2$, are the solutions of the saddle-point equations:

$$\frac{\partial \mathcal{W}(\mathbf{z}_f, \mathbf{E})}{\partial E_\mu} = 0 \Leftrightarrow \frac{2\eta_1}{E_\mu} + \frac{2\eta_2}{E_\mu - x} + \frac{2\eta_3}{E_\mu - 1} + \sum_{\substack{\nu=1 \\ \nu \neq \mu}}^M \frac{2}{E_\mu - E_\nu} = 0$$

$$\tag{6.7}$$

where $\mu = 1, \dots, M$. In [25], relation (6.6) was verified in the simplest cases—namely $M_1 = M_2 = 1$ and $\hat{\alpha}_1 = \hat{\alpha}_2 = \hat{\alpha}_3 = b\eta$ —using elementary Mathematica routines. A more detailed numerical analysis is required to explore the analytic structure of the classical block. This example is not unique: a similar correspondence ties WZW and Virasoro torus blocks to the Bethe ansatz solution of the elliptic Calogero–Moser model [26–28].¹⁴ One of

¹⁴In the case of the torus one-point Virasoro block, a rigorous proof establishes the equivalence between its integral representation and its power series expansion [29]. This result was then leveraged within the probabilistic framework to give a fully rigorous construction of the torus one-point block and to prove the existence of its classical limit [30].

our main motivations in developing a numerical solver for Bethe equations in RG models was to explore these connections. We will present the analytical and numerical results on these correspondences in a forthcoming paper.

7 Conclusions and outlook

The present work has begun with a review of classical and quantum integrability, together with an introduction to the Richardson reduced BCS and Gaudin central spin models. To ensure the paper’s self-sufficiency, every derivation concerning Richardson’s solution has been presented in full detail, providing a comprehensive reference for readers new to the subject. Building on this foundation, we have reexamined the well-established correspondence between Richardson–Gaudin models and two-dimensional conformal field theory and have identified the appearance of irregular, degenerate Virasoro blocks within this framework.

Our principal achievement is the development of a numerical solver for the Bethe equations in Richardson–Gaudin models. Our numerical experiments confirm that the implementation yields accurate rapidity trajectories. Of particular note is the observation that the rapidity trajectories are invariant with respect to scaling—a property with potentially profound practical and physical implications that deserves further investigation. A possible direction for future research is to leverage the electrostatic analogy to design novel and more robust numerical methods for computing rapidities.¹⁵

We have also described an extension of our method to finite temperatures, introducing a scheme for directly computing temperature-dependent pairing energies and other thermodynamic observables within the discrete Richardson model. It would be interesting to re-examine time-dependent extensions of the Richardson–Gaudin models and to explore their potential connections with the 2D CFT framework. Such a correspondence appears plausible, especially in view of the formulation in terms of the Yang–Yang function (see e.g. [31] and refs. therein).

This work adopts a standard analytical-numerical perspective, combining Bethe ansatz techniques with computational tools to study Richardson–Gaudin integrable models. However, our broader program envisions three complementary directions for future exploration:

1. *Matrix model perspective.*

One first observes that, in the thermodynamic limit $L, M \rightarrow \infty$ with fixed filling

¹⁵Indeed, one can interpret the E_ν as mobile unit charges that repel each other via a logarithmic Coulomb interaction, while being attracted to fixed background charges located at the ϵ_j . The variational condition $\nabla \mathcal{W}^R(\{E_\nu\}) = 0$ then corresponds to finding the electrostatic equilibrium configuration of this charge system. This physical picture naturally suggests alternative numerical strategies. In particular, modern gradient-based optimization algorithms—especially when combined with automatic differentiation and appropriate “soft-core” regularization to avoid numerical singularities when $E_\mu \approx E_\nu$ —provide a promising alternative to traditional Newton–Raphson or Laguerre solvers. Such methods may offer improved robustness, better convergence behavior, and scalability to large systems.

fraction M/L , the Bethe rapidities $\{E_\nu\}$ condense onto continuous arcs in the complex plane (cf. [32]). These arcs are described by a spectral density $\rho(E)$ supported on a hyperelliptic curve—mirroring the large- N behavior of Hermitian one-matrix model, where eigenvalues form cuts on a similar curve via loop (saddle-point) equations [33, 34].

Moreover, a precise identification follows: the Bethe roots coincide with the zeros of the Baxter polynomial (4.2), which itself satisfies a second order differential equation. In the semiclassical (large- N) limit, this differential equation reproduces the spectral curve of the corresponding matrix model.

An interesting problem is to establish this Bethe ansatz \leftrightarrow matrix model mapping rigorously for integrable pairing models and to assess its practical utility. Encouragingly, known results for Gaudin-type models (see [35]) suggest this program is within reach.

2. Advanced techniques from 2D CFT.

The appearance of Gaiotto–Witten irregular, degenerate conformal blocks in the structure of the Richardson Yang–Yang function opens a path to apply powerful tools from 2D CFT. Our primary objective is to exploit the BPZ differential equations satisfied by these blocks to derive—via their classical (large- c) limit and a subsequent saddle-point analysis—the equations for the critical Richardson Yang–Yang function $\mathcal{W}_{\text{crit}}^R$. Moreover, the Gaiotto–Witten irregular blocks featured here have recently attracted renewed attention due to their connection with a novel class of integrable systems (see [19, 20]). It would be highly worthwhile to investigate how these emerging structures relate to—and potentially enrich—the Richardson–Gaudin models.

It would also be interesting to examine the RG models from the perspective of the matrix model (β -ensemble)/2D CFT correspondence developed in [36].

3. Connections with 4D gauge theories.

Through the AGT [37] and Bethe/gauge [38] correspondences, Richardson–Gaudin systems may also find reinterpretation in terms of four-dimensional $\mathcal{N} = 2$ supersymmetric gauge theories. These theories provide a unifying framework for linking matrix models, integrable systems, and 2D CFT. For example, the Seiberg–Witten curves—analogs of matrix model spectral curves—and their quantum deformations naturally encode the spectra of quantum integrable systems, suggesting a bridge between $\mathcal{N} = 2$ gauge theories and Richardson–Gaudin models.

Acknowledgements

The research presented here has been supported by the Polish National Science Centre under grant no. 2023/49/B/ST2/01371.

A Derivation of the Poisson bracket of Lax matrices

We aim to compute the Poisson bracket of Lax matrices:

$$\{L_1, L_2\} = [r_{12}, L_1] - [r_{21}, L_2],$$

where $L = U\Lambda U^{-1}$ is the Lax matrix, with Λ being a diagonal matrix of eigenvalues and U a matrix of eigenvectors.

We begin by evaluating:

$$\{L_1, L_2\} = \{U_1\Lambda_1 U_1^{-1}, U_2\Lambda_2 U_2^{-1}\}.$$

Applying the Leibniz rule:

$$\begin{aligned} \{L_1, L_2\} &= \{U_1\Lambda_1 U_1^{-1}, U_2\Lambda_2 U_2^{-1}\} \\ &= U_1\{\Lambda_1 U_1^{-1}, U_2\Lambda_2 U_2^{-1}\} + \{U_1, U_2\Lambda_2 U_2^{-1}\}\Lambda_1 U_1^{-1}. \end{aligned}$$

Expanding all brackets using the Leibniz and chain rules, we obtain a sum of nine terms. To simplify the expression, we define:

$$\begin{aligned} k_{12} &\equiv \{U_1, U_2\}U_1^{-1}U_2^{-1}, & k_{21} &\equiv \{U_2, U_1\}U_2^{-1}U_1^{-1}, \\ q_{12} &\equiv U_2\{U_1, \Lambda_2\}U_2^{-1}U_1^{-1}, & q_{21} &\equiv U_1\{U_2, \Lambda_1\}U_1^{-1}U_2^{-1}. \end{aligned}$$

Note that $k_{12} = -k_{21}$, while no such relation generally holds between q_{12} and q_{21} . We also use the identity:

$$\{A_1, B_2^{-1}\} = B_2^{-1}\{A_1, B_2\}B_2^{-1},$$

which follows from $\{A_1, B_2^{-1}B_2\} = 0$. Now we compute each term in the Poisson bracket:

1. $U_1\Lambda_1 U_2\Lambda_2\{U_1^{-1}, U_2^{-1}\} = L_1 L_2 k_{12}$
2. $U_1\Lambda_1 U_2\{U_1^{-1}, \Lambda_2\}U_2^{-1} = -L_1 q_{12}$
3. $U_1\Lambda_1\{U_1^{-1}, U_2\}\Lambda_2 U_2^{-1} = -L_1 k_{12} L_2$
4. $U_1 U_2 \Lambda_2\{\Lambda_1, U_2^{-1}\}U_1^{-1} = L_2 q_{21}$
5. $\{\Lambda_1, \Lambda_2\} = 0$
6. $U_1\{\Lambda_1, U_2\}\Lambda_2 U_2^{-1}U_1^{-1} = -q_{21} L_2$

$$7. U_2 \Lambda_2 \{U_1, U_2^{-1}\} \Lambda_1 U_1^{-1} = -L_2 k_{12} L_1$$

$$8. U_2 \{U_1, \Lambda_2\} U_2^{-1} \Lambda_1 U_1^{-1} = q_{12} L_1$$

$$9. \{U_1, U_2\} \Lambda_2 U_2^{-1} \Lambda_1 U_1^{-1} = k_{12} L_2 L_1$$

Combining all the terms:

$$\begin{aligned} \{L_1, L_2\} &= L_1 L_2 k_{12} - L_1 q_{12} - L_1 k_{12} L_2 + L_2 q_{21} - q_{21} L_2 \\ &\quad - L_2 k_{12} L_1 + q_{12} L_1 + k_{12} L_2 L_1. \end{aligned}$$

Rewriting and grouping:

$$\begin{aligned} \{L_1, L_2\} &= L_1 [L_2, k_{12}] + [q_{12}, L_1] + [L_2, q_{21}] - [L_2, k_{12}] L_1 \\ &= [L_1, [L_2, k_{12}]] + [q_{12}, L_1] - [q_{21}, L_2]. \end{aligned}$$

By the Jacobi identity:

$$[[k_{12}, L_2], L_1] + [[L_1, k_{12}], L_2] + [[L_2, L_1], k_{12}] = 0.$$

Since $[L_1, L_2] = 0$, it follows:

$$[[k_{12}, L_2], L_1] = -[[L_1, k_{12}], L_2] = -[[k_{21}, L_1], L_2].$$

Thus,

$$\begin{aligned} \{L_1, L_2\} &= \frac{1}{2} [[k_{12}, L_2], L_1] - \frac{1}{2} [[k_{21}, L_1], L_2] + [q_{12}, L_1] - [q_{21}, L_2] \\ &= \left[q_{12} + \frac{1}{2} [k_{12}, L_2], L_1 \right] - \left[q_{21} + \frac{1}{2} [k_{21}, L_1], L_2 \right]. \end{aligned}$$

We define the classical r -matrix as:

$$r_{ij} \equiv q_{ij} + \frac{1}{2} [k_{ij}, L_j],$$

so the Poisson bracket becomes:

$$\boxed{\{L_1, L_2\} = [r_{12}, L_1] - [r_{21}, L_2].}$$

B Hard-core boson algebra

Commutator $[b_i, b_j^\dagger]$

For the off-diagonal case $i \neq j$, one finds

$$\begin{aligned} [b_i, b_j^\dagger] &= b_i b_j^\dagger - b_j^\dagger b_i = b_i b_j^\dagger - c_{j+}^\dagger c_{j-}^\dagger c_{i-} c_{i+} = b_i b_j^\dagger + c_{j+}^\dagger c_{i-} c_{j-}^\dagger c_{i+} \\ &= b_i b_j^\dagger - c_{i-} c_{j+}^\dagger c_{j-}^\dagger c_{i+} = b_i b_j^\dagger + c_{i-} c_{j+}^\dagger c_{i+} c_{j-}^\dagger = b_i b_j^\dagger - c_{i-} c_{i+} c_{j+}^\dagger c_{j-}^\dagger \end{aligned}$$

$$= b_i b_j^\dagger - b_i^\dagger b_j = 0. \quad (\text{B.1})$$

When $i = j$, one obtains

$$\begin{aligned} [b_i, b_i^\dagger] &= b_i b_i^\dagger - b_i^\dagger b_i = b_i b_i^\dagger - c_{i+}^\dagger c_{i-}^\dagger c_{i-} c_{i+} = b_i b_i^\dagger - c_{i+}^\dagger (1 - c_{i-} c_{i-}^\dagger) c_{i+} \\ &= b_i b_i^\dagger - c_{i+}^\dagger c_{i+} + c_{i+}^\dagger c_{i-} c_{i-}^\dagger c_{i+} = b_i b_i^\dagger - c_{i+}^\dagger c_{i+} - c_{i-} c_{i+}^\dagger c_{i-}^\dagger c_{i+} \\ &= b_i b_i^\dagger - c_{i+}^\dagger c_{i+} + c_{i-} c_{i+}^\dagger c_{i+} c_{i-}^\dagger = b_i b_i^\dagger - c_{i+}^\dagger c_{i+} + c_{i-} (1 - c_{i+} c_{i+}^\dagger) c_{i-}^\dagger \\ &= b_i b_i^\dagger - c_{i+}^\dagger c_{i+} + c_{i-} c_{i-}^\dagger - c_{i-} c_{i+} c_{j+}^\dagger c_{i-}^\dagger = b_i b_i^\dagger - c_{i+}^\dagger c_{i+} + c_{i-} c_{i-}^\dagger - b_i b_i^\dagger \\ &= c_{i-} c_{i-}^\dagger - c_{i+}^\dagger c_{i+} = 1 - c_{i-}^\dagger c_{i-} - c_{i+}^\dagger c_{i+}. \end{aligned} \quad (\text{B.2})$$

Finally, consider the operator

$$\hat{n}_{i-} + \hat{n}_{i+} = c_{i-}^\dagger c_{i-} + c_{i+}^\dagger c_{i+}$$

acting on a given many-body state. Since we restrict our attention to either fully occupied or completely empty levels, each number operator $c_{i\sigma}^\dagger c_{i\sigma}$ simply measures the occupancy of the single particle state $|i, \sigma\rangle$. In a fully occupied level $|i, -\rangle$ and $|i, +\rangle$, both \hat{n}_{i-} and \hat{n}_{i+} return 1. Conversely, on an empty level they each return 0. Thus $\hat{n}_{i-} + \hat{n}_{i+}$ equals 2 for a doubly occupied site and 0 for an unoccupied site.

The operator $b_i^\dagger b_i$ refers to the number of Cooper pairs, which occupy certain energy level ϵ_i . This means that for fully occupied or non-occupied level, we have

$$c_{i-}^\dagger c_{i-} + c_{i+}^\dagger c_{i+} = 2b_i^\dagger b_i \Rightarrow [b_i, b_i^\dagger] = 1 - 2b_i^\dagger b_i. \quad (\text{B.3})$$

Combining both cases, we obtain

$$[b_i, b_j^\dagger] = \delta_{ij} (1 - 2b_i^\dagger b_i). \quad (\text{B.4})$$

Commutator $[b_i^\dagger b_i, b_j^\dagger]$

First, let us consider the commutator $[b_i^\dagger, b_j^\dagger]$:

$$\begin{aligned} [b_i^\dagger, b_j^\dagger] &= b_i^\dagger b_j^\dagger - b_j^\dagger b_i^\dagger = b_i^\dagger b_j^\dagger - c_{j+}^\dagger c_{j-}^\dagger c_{i+}^\dagger c_{i-}^\dagger = b_i^\dagger b_j^\dagger + c_{j+}^\dagger c_{i+}^\dagger c_{j-}^\dagger c_{i-}^\dagger \\ &= b_i^\dagger b_j^\dagger - c_{i+}^\dagger c_{j+}^\dagger c_{j-}^\dagger c_{i-}^\dagger = b_i^\dagger b_j^\dagger + c_{i+}^\dagger c_{j+}^\dagger c_{i-}^\dagger c_{j-}^\dagger = b_i^\dagger b_j^\dagger - c_{i+}^\dagger c_{i-}^\dagger c_{j+}^\dagger c_{j-}^\dagger \\ &= b_i^\dagger b_j^\dagger - b_i^\dagger b_j^\dagger = 0 \Rightarrow b_i^\dagger b_j^\dagger = b_j^\dagger b_i^\dagger. \end{aligned} \quad (\text{B.5})$$

Using this result, let us first compute the commutator $[b_i^\dagger b_i, b_j^\dagger]$ in the case $i \neq j$:

$$[b_i^\dagger b_i, b_j^\dagger] = b_i^\dagger b_i b_j^\dagger - b_j^\dagger b_i^\dagger b_i = b_i^\dagger b_i b_j^\dagger - b_i^\dagger b_j^\dagger b_i = b_i^\dagger b_i b_j^\dagger - b_i^\dagger b_i b_j^\dagger = 0. \quad (\text{B.6})$$

When $i = j$, we have

$$[b_i^\dagger b_i, b_i^\dagger] = b_i^\dagger b_i b_i^\dagger - b_i^\dagger b_i^\dagger b_i = b_i^\dagger (1 - 2b_i^\dagger b_i + b_i^\dagger b_i) - (b_i^\dagger)^2 b_i$$

$$= b_i^\dagger - b_i^\dagger b_i^\dagger b_i = b_i^\dagger - \left(b_i^\dagger \right)^2 b_i = b_i^\dagger. \quad (\text{B.7})$$

Combining these two results, we get

$$\left[b_i^\dagger b_i, b_j^\dagger \right] = \delta_{ij} b_i^\dagger. \quad (\text{B.8})$$

C Derivation of the Richardson equations

Let us consider the eigenvalue problem for the Hamiltonian (3.6):

$$H_{\mathcal{U}} |\Psi_M\rangle_{\mathcal{U}} = \mathbb{E}(M) |\Psi_M\rangle_{\mathcal{U}}. \quad (\text{C.1})$$

We will use the Bethe ansatz in the form

$$|\Psi_M\rangle_{\mathcal{U}} = \prod_{\nu=1}^M B_\nu^\dagger |0\rangle, \quad (\text{C.2})$$

where

$$B_\nu^\dagger = \sum_{j \in \mathcal{U}} \frac{b_j^\dagger}{2\epsilon_j - E_\nu}, \quad \left[b_j^\dagger b_j, B_\nu^\dagger \right] = \frac{b_j^\dagger}{2\epsilon_j - E_\nu}. \quad (\text{C.3})$$

The eigenvalue problem can be rewritten as

$$H_{\mathcal{U}} \prod_{\nu=1}^M B_\nu^\dagger |0\rangle = \mathbb{E}(M) \prod_{\nu=1}^M B_\nu^\dagger |0\rangle. \quad (\text{C.4})$$

Since $H_{\mathcal{U}} |0\rangle = 0$, we have

$$\left[H_{\mathcal{U}}, \prod_{\nu=1}^M B_\nu^\dagger \right] |0\rangle = H_{\mathcal{U}} \prod_{\nu=1}^M B_\nu^\dagger |0\rangle - \prod_{\nu=1}^M B_\nu^\dagger H_{\mathcal{U}} |0\rangle = H_{\mathcal{U}} \prod_{\nu=1}^M B_\nu^\dagger |0\rangle. \quad (\text{C.5})$$

We can also show that the commutator of an operator with a product of operators is generally given by

$$\left[A, \prod_{\nu=1}^M B_\nu \right] = \sum_{\nu=1}^M \left(\prod_{\eta=1}^{\nu-1} B_\eta \right) [A, B_\nu] \left(\prod_{\mu=\nu+1}^M B_\mu \right). \quad (\text{C.6})$$

Consequently, equation (C.4) can be rewritten in the form

$$H_{\mathcal{U}} |\Psi_M\rangle_{\mathcal{U}} = \sum_{\nu=1}^M \left(\prod_{\eta=1}^{\nu-1} B_\eta^\dagger \right) \left[H_{\mathcal{U}}, B_\nu^\dagger \right] \left(\prod_{\mu=\nu+1}^M B_\mu^\dagger \right) |0\rangle. \quad (\text{C.7})$$

To find the commutator $[H_{\mathcal{U}}, B_\nu^\dagger]$, we introduce the following collective operators:

$$B_0^\dagger = \sum_{j \in \mathcal{U}} b_j^\dagger, \quad B_0 = \sum_{j \in \mathcal{U}} b_j. \quad (\text{C.8})$$

Accordingly, the Hamiltonian $H_{\mathcal{U}}$ can be written as

$$\begin{aligned} H_{\mathcal{U}} &= \sum_{j \in \mathcal{U}} 2\epsilon_j b_j^\dagger b_j - g \sum_{i,j \in \mathcal{U}} b_i^\dagger b_j = \sum_{j \in \mathcal{U}} 2\epsilon_j b_j^\dagger b_j - g \sum_{i \in \mathcal{U}} b_i^\dagger \sum_{j \in \mathcal{U}} b_j \\ &= \sum_{j \in \mathcal{U}} 2\epsilon_j b_j^\dagger b_j - g B_0^\dagger B_0. \end{aligned} \quad (\text{C.9})$$

For simplicity, we first compute the commutators $[B_0, B_\nu^\dagger]$ and $[B_0^\dagger, B_\nu^\dagger]$:

$$\begin{aligned} [B_0, B_\nu^\dagger] &= B_0 B_\nu^\dagger - \nu^\dagger B_0 = \sum_{i \in \mathcal{U}} b_i \sum_{j \in \mathcal{U}} \frac{b_j^\dagger}{2\epsilon_j - E_\nu} - \sum_{j \in \mathcal{U}} \frac{b_j^\dagger}{2\epsilon_j - E_\nu} \sum_{i \in \mathcal{U}} b_i \\ &= \sum_{i,j \in \mathcal{U}} \frac{b_i b_j^\dagger}{2\epsilon_j - E_\nu} - \sum_{i,j \in \mathcal{U}} \frac{b_j^\dagger b_i}{2\epsilon_j - E_\nu} = \sum_{i,j \in \mathcal{U}} \frac{b_i b_j^\dagger - b_j^\dagger b_i}{2\epsilon_j - E_\nu} = \sum_{i,j \in \mathcal{U}} \frac{[b_i, b_j^\dagger]}{2\epsilon_j - E_\nu} \\ &= \sum_{i,j \in \mathcal{U}} \frac{\delta_{ij} (1 - 2b_i^\dagger b_i)}{2\epsilon_j - E_\nu} = \sum_{j \in \mathcal{U}} \frac{1 - 2b_j^\dagger b_j}{2\epsilon_j - E_\nu}, \end{aligned} \quad (\text{C.10})$$

and

$$\begin{aligned} [B_0^\dagger, B_\nu^\dagger] &= B_0^\dagger B_\nu^\dagger - B_\nu^\dagger B_0^\dagger = \sum_{i \in \mathcal{U}} b_i^\dagger \sum_{j \in \mathcal{U}} \frac{b_j^\dagger}{2\epsilon_j - E_\nu} - \sum_{j \in \mathcal{U}} \frac{b_j^\dagger}{2\epsilon_j - E_\nu} \sum_{i \in \mathcal{U}} b_i^\dagger \\ &= \sum_{i,j \in \mathcal{U}} \frac{b_i^\dagger b_j^\dagger - b_j^\dagger b_i^\dagger}{2\epsilon_j - E_\nu} = \sum_{i,j \in \mathcal{U}} \frac{[b_i^\dagger, b_j^\dagger]}{2\epsilon_j - E_\nu} = 0. \end{aligned} \quad (\text{C.11})$$

Therefore, the commutator $[H_{\mathcal{U}}, B_\nu^\dagger]$ is

$$\begin{aligned} [H_{\mathcal{U}}, B_\nu^\dagger] &= \left[\sum_{i \in \mathcal{U}} 2\epsilon_i b_i^\dagger b_i - g B_0^\dagger B_0, B_\nu^\dagger \right] = \left[\sum_{i \in \mathcal{U}} 2\epsilon_i b_i^\dagger b_i, B_\nu^\dagger \right] - \left[g B_0^\dagger B_0, B_\nu^\dagger \right] \\ &= \sum_{i \in \mathcal{U}} 2\epsilon_i [b_i^\dagger b_i, B_\nu^\dagger] - g B_0^\dagger [B_0, B_\nu^\dagger] - g [B_0^\dagger, B_\nu^\dagger] B_0 \\ &= \sum_{i \in \mathcal{U}} 2\epsilon_i \left(\frac{b_i^\dagger}{2\epsilon_i - E_\nu} \right) - g B_0^\dagger \sum_{i \in \mathcal{U}} \frac{1 - 2b_i^\dagger b_i}{2\epsilon_i - E_\nu} \\ &= \sum_{i \in \mathcal{U}} \frac{(2\epsilon_i - E_\nu + E_\nu) b_i^\dagger}{2\epsilon_i - E_\nu} - g B_0^\dagger \sum_{i \in \mathcal{U}} \frac{1 - 2b_i^\dagger b_i}{2\epsilon_i - E_\nu} \\ &= E_\nu \sum_{i \in \mathcal{U}} \frac{b_i^\dagger}{2\epsilon_i - E_\nu} + \sum_{i \in \mathcal{U}} \frac{(2\epsilon_i - E_\nu) b_i^\dagger}{2\epsilon_i - E_\nu} - g B_0^\dagger \sum_{i \in \mathcal{U}} \frac{1 - 2b_i^\dagger b_i}{2\epsilon_i - E_\nu} \\ &= E_\nu B_\nu^\dagger + \sum_{i \in \mathcal{U}} b_i^\dagger - g B_0^\dagger \sum_{i \in \mathcal{U}} \frac{1 - 2b_i^\dagger b_i}{2\epsilon_i - E_\nu} \\ &= E_\nu B_\nu^\dagger + B_0^\dagger - g B_0^\dagger \sum_{i \in \mathcal{U}} \frac{1 - 2b_i^\dagger b_i}{2\epsilon_i - E_\nu} = E_\nu B_\nu^\dagger + B_0^\dagger \left[1 - g \sum_{i \in \mathcal{U}} \frac{1 - 2b_i^\dagger b_i}{2\epsilon_i - E_\nu} \right]. \end{aligned} \quad (\text{C.12})$$

Substituting this result into (C.7) yields

$$\begin{aligned}
& \sum_{\nu=1}^M \left(\prod_{\eta=1}^{\nu-1} B_\eta^\dagger \right) \left\{ E_\nu B_\nu^\dagger + B_0^\dagger \left[1 - g \sum_{j \in \mathcal{U}} \frac{1 - 2b_j^\dagger b_j}{2\epsilon_j - E_\nu} \right] \right\} \left(\prod_{\mu=\nu+1}^M B_\mu^\dagger \right) |0\rangle \\
&= \sum_{\nu=1}^M \left(\prod_{\eta=1}^{\nu-1} B_\eta^\dagger \right) E_\nu B_\nu^\dagger \left(\prod_{\mu=\nu+1}^M B_\mu^\dagger \right) |0\rangle + \sum_{\nu=1}^M \left(\prod_{\eta=1}^{\nu-1} B_\eta^\dagger \right) B_0^\dagger \left(\prod_{\mu=\nu+1}^M B_\mu^\dagger \right) |0\rangle \\
&\quad - \sum_{\nu=1}^M \left(\prod_{\eta=1}^{\nu-1} B_\eta^\dagger \right) B_0^\dagger \sum_{j \in \mathcal{U}} \frac{g}{2\epsilon_j - E_\nu} \left(\prod_{\mu=\nu+1}^M B_\mu^\dagger \right) |0\rangle \\
&\quad + \sum_{\nu=1}^M \left(\prod_{\eta=1}^{\nu-1} B_\eta^\dagger \right) \sum_{j \in \mathcal{U}} \frac{2gB_0^\dagger b_j^\dagger b_j}{2\epsilon_j - E_\nu} \left(\prod_{\mu=\nu+1}^M B_\mu^\dagger \right) |0\rangle. \tag{C.13}
\end{aligned}$$

Let us examine this expression term by term. The first term is

$$\begin{aligned}
& \sum_{\nu=1}^M E_\nu \left(\prod_{\eta=1}^{\nu-1} B_\eta^\dagger \right) B_\nu^\dagger \left(\prod_{\mu=\nu+1}^M B_\mu^\dagger \right) |0\rangle = \sum_{\nu=1}^M E_\nu \prod_{\nu=1}^M B_\nu^\dagger |0\rangle \\
&= \sum_{\nu=1}^M E_\nu |\Psi_M\rangle_{\mathcal{U}} = \mathbb{E}(M) |\Psi_M\rangle_{\mathcal{U}}. \tag{C.14}
\end{aligned}$$

Since $[B_0^\dagger, B_J^\dagger] = 0$, we may pull B_0^\dagger outside in the second term, which yields

$$\sum_{\nu=1}^M B_0^\dagger \left(\prod_{\eta=1}^M B_\eta^\dagger \right) \left(\prod_{\mu=\nu+1}^M B_\mu^\dagger \right) |0\rangle = \sum_{\nu=1}^M B_0^\dagger \left(\prod_{\mu \neq \nu}^M B_\mu^\dagger \right) |0\rangle. \tag{C.15}$$

The third term reduces to

$$\sum_{\nu=1}^M \left(\prod_{\eta=1}^{\nu-1} B_\eta^\dagger \right) \sum_{j \in \mathcal{U}} \frac{g}{2\epsilon_j - E_\nu} \left(\prod_{\mu=\nu+1}^M B_\mu^\dagger \right) |0\rangle = \sum_{\nu=1}^M \sum_{j \in \mathcal{U}} \frac{g}{2\epsilon_j - E_\nu} \left(\prod_{\mu \neq \nu}^M B_\mu^\dagger \right) |0\rangle, \tag{C.16}$$

which can then be combined with the second term to yield

$$\sum_{\nu=1}^M B_0^\dagger \left[1 - \sum_{j \in \mathcal{U}} \frac{g}{2\epsilon_j - E_\nu} \right] \left(\prod_{\mu \neq \nu}^M B_\mu^\dagger \right) |0\rangle. \tag{C.17}$$

Finally, let us evaluate the last term by first considering the following commutator:

$$\begin{aligned}
\left[\sum_{j \in \mathcal{U}} \frac{2gB_0^\dagger b_j^\dagger b_j}{2\epsilon_j - E_\nu}, B_\mu^\dagger \right] &= \sum_{j \in \mathcal{U}} \frac{2gB_0^\dagger b_j^\dagger b_j}{2\epsilon_j - E_\nu} B_\mu^\dagger - B_\mu^\dagger \sum_{j \in \mathcal{U}} \frac{2gB_0^\dagger b_j^\dagger b_j}{2\epsilon_j - E_\nu} \\
&= \sum_{j \in \mathcal{U}} \frac{(2gB_0^\dagger b_j^\dagger b_j B_\mu^\dagger) - (2gB_\mu^\dagger B_0^\dagger b_j^\dagger b_j)}{2\epsilon_j - E_\mu}
\end{aligned}$$

$$\begin{aligned}
&= \sum_{j \in \mathcal{U}} \frac{\left(2gB_0^\dagger b_j^\dagger b_j B_\mu^\dagger\right) - \left(2gB_0^\dagger B_\mu^\dagger b_j^\dagger b_j\right)}{2\epsilon_j - E_\mu} \\
&= \sum_{j \in \mathcal{U}} \frac{2gB_0^\dagger [b_j^\dagger b_j, B_\nu^\dagger]}{2\epsilon_j - E_\nu} \\
&= \sum_{j \in \mathcal{U}} \frac{2gB_0^\dagger}{2\epsilon_j - E_\nu} \frac{b_j^\dagger}{2\epsilon_i - E_\mu} \\
&= 2gB_0^\dagger \sum_{j \in \mathcal{U}} \frac{b_j^\dagger (E_\nu - E_\mu)}{(2\epsilon_j - E_\nu)(2\epsilon_j - E_\mu)(E_\nu - E_\mu)} \\
&= 2gB_0^\dagger \sum_{j \in \mathcal{U}} \frac{b_j^\dagger (2\epsilon_j - E_\mu) - b_j^\dagger (2\epsilon_j - E_\nu)}{(2\epsilon_j - E_\nu)(2\epsilon_j - E_\mu)(E_\nu - E_\mu)} \\
&= 2gB_0^\dagger \sum_{j \in \mathcal{U}} \left(\frac{b_j^\dagger}{(2\epsilon_j - E_\nu)(E_\nu - E_\mu)} - \frac{b_j^\dagger}{(2\epsilon_j - E_\mu)(E_\nu - E_\mu)} \right) \\
&= 2gB_0^\dagger \frac{B_\nu^\dagger - B_\mu^\dagger}{E_\nu - E_\mu}. \tag{C.18}
\end{aligned}$$

This leads us to conclude that

$$\begin{aligned}
&\left[\sum_{j \in \mathcal{U}} \frac{2gB_0^\dagger b_j^\dagger b_j}{2\epsilon_j - E_\nu}, \prod_{\mu=\nu+1}^M B_\mu^\dagger \right] = \sum_{\mu=\nu+1}^M \left(\prod_{\eta'=\nu+1}^{\mu-1} B_{J_{\eta'}}^\dagger \right) \left[\sum_{j \in \mathcal{U}} \frac{2gB_0^\dagger b_j^\dagger b_j}{2\epsilon_j - E_\nu}, B_\mu^\dagger \right] \\
&\times \left(\prod_{\mu'=\mu+1}^M B_{J_{\mu'}}^\dagger \right) = \sum_{\mu=\nu+1}^M \left(\prod_{\eta'=\nu+1}^{\mu-1} B_{J_{\eta'}}^\dagger \right) 2gB_0^\dagger \frac{B_{\nu^\dagger} - B_\mu^\dagger}{E_\nu - E_\mu} \left(\prod_{\mu'=\mu+1}^M B_{J_{\mu'}}^\dagger \right) \\
&= \sum_{\mu=\nu+1}^M \left(\prod_{\eta'=\nu+1}^{\mu-1} B_{J_{\eta'}}^\dagger \right) \frac{2gB_0^\dagger B_{\nu^\dagger}}{E_\nu - E_\mu} \left(\prod_{\mu'=\mu+1}^M B_{J_{\mu'}}^\dagger \right) \\
&- \sum_{\mu=\nu+1}^M \left(\prod_{\eta'=\nu+1}^{\mu-1} B_{J_{\eta'}}^\dagger \right) \frac{2gB_0^\dagger B_{\mu^\dagger}}{E_\nu - E_\mu} \left(\prod_{\mu'=\mu+1}^M B_{J_{\mu'}}^\dagger \right) \\
&= \sum_{\mu=\nu+1}^M \frac{2gB_0^\dagger}{E_\nu - E_\mu} \left(\prod_{\eta'=\nu+1}^{\mu-1} B_{J_{\eta'}}^\dagger \right) B_\nu^\dagger \left(\prod_{\mu'=\mu+1}^M B_{J_{\mu'}}^\dagger \right) \\
&- \sum_{\mu=\nu+1}^M \frac{2gB_0^\dagger}{E_\nu - E_\mu} \left(\prod_{\eta'=\nu+1}^{\mu-1} B_{J_{\eta'}}^\dagger \right) B_\mu^\dagger \left(\prod_{\mu'=\mu+1}^M B_{J_{\mu'}}^\dagger \right). \tag{C.19}
\end{aligned}$$

Observe that the same commutator can also be expressed as

$$\left[\sum_{j \in \mathcal{U}} \frac{2gB_0^\dagger b_j^\dagger b_j}{2\epsilon_j - E_\nu}, \prod_{\mu=\nu+1}^M B_\mu^\dagger \right] = \sum_{j \in \mathcal{U}} \frac{2gB_0^\dagger b_j^\dagger b_j}{2\epsilon_j - E_\nu} \left(\prod_{\mu=\nu+1}^M B_\mu^\dagger \right)$$

$$\begin{aligned}
& - \left(\prod_{\mu=\nu+1}^M B_\mu^\dagger \right) \sum_{j \in \mathcal{U}} \frac{2gB_0^\dagger b_j^\dagger b_j}{2\epsilon_j - E_\nu} \Rightarrow \\
& \left[\sum_{j \in \mathcal{U}} \frac{2gB_0^\dagger b_j^\dagger b_j}{2\epsilon_j - E_\nu}, \prod_{\mu=\nu+1}^M B_\mu^\dagger \right] |0\rangle = \sum_{j \in \mathcal{U}} \frac{2gB_0^\dagger b_j^\dagger b_j}{2\epsilon_j - E_\nu} \left(\prod_{\mu=\nu+1}^M B_\mu^\dagger \right) |0\rangle. \quad (C.20)
\end{aligned}$$

This means that our last term of (C.13) can be written as

$$\begin{aligned}
& \sum_{\nu=1}^M \left(\prod_{\eta=1}^{\nu-1} B_\eta^\dagger \right) \left[\sum_{j \in \mathcal{U}} \frac{2gB_0^\dagger b_j^\dagger b_j}{2\epsilon_j - E_\nu}, \prod_{\mu=\nu+1}^M B_\mu^\dagger \right] |0\rangle \\
& = \sum_{\nu=1}^M \left[\sum_{\mu=\nu+1}^M \frac{2gB_0^\dagger}{E_\nu - E_\mu} \left(\prod_{\eta=1}^{\nu-1} B_\eta^\dagger \right) \left(\prod_{\eta'=\nu+1}^{\mu-1} B_{J_{\eta'}}^\dagger \right) B_\nu^\dagger \left(\prod_{\mu'=\mu+1}^M B_{J_{\mu'}}^\dagger \right) \right] |0\rangle \\
& - \sum_{\nu=1}^M \left[\sum_{\mu=\nu+1}^M \frac{2gB_0^\dagger}{E_\nu - E_\mu} \left(\prod_{\eta=1}^{\nu-1} B_\eta^\dagger \right) \left(\prod_{\eta'=\nu+1}^{\mu-1} B_{J_{\eta'}}^\dagger \right) B_\mu^\dagger \left(\prod_{\mu'=\mu+1}^M B_{J_{\mu'}}^\dagger \right) \right] |0\rangle \\
& = \sum_{\nu=1}^M \left[\sum_{\mu=\nu+1}^M \frac{2gB_0^\dagger}{E_\nu - E_\mu} \left(\prod_{\eta \neq \mu}^M B_\eta^\dagger \right) \right] |0\rangle - \sum_{\nu=1}^M \left[\sum_{\mu=\nu+1}^M \frac{2gB_0^\dagger}{E_\nu - E_\mu} \left(\prod_{\eta \neq \nu}^M B_\eta^\dagger \right) \right] |0\rangle \\
& = \sum_{\mu=1}^M \left[\sum_{\nu=1}^{\mu-1} \frac{2gB_0^\dagger}{E_\nu - E_\mu} \right] \left(\prod_{\eta \neq \mu}^M B_\eta^\dagger \right) |0\rangle - \sum_{\nu=1}^M \left[\sum_{\mu=\nu+1}^M \frac{2gB_0^\dagger}{E_\nu - E_\mu} \right] \left(\prod_{\eta \neq \nu}^M B_\eta^\dagger \right) |0\rangle \\
& = \sum_{\nu=1}^M \left[\sum_{\mu=1}^{\nu-1} \frac{2gB_0^\dagger}{E_\mu - E_\nu} \right] \left(\prod_{\eta \neq \nu}^M B_\eta^\dagger \right) |0\rangle - \sum_{\nu=1}^M \left[\sum_{\mu=\nu+1}^M \frac{2gB_0^\dagger}{E_\nu - E_\mu} \right] \left(\prod_{\eta \neq \nu}^M B_\eta^\dagger \right) |0\rangle \\
& = \sum_{\nu=1}^M \left[\sum_{\mu=1}^{\nu-1} \frac{2gB_0^\dagger}{E_\mu - E_\nu} + \sum_{\mu=\nu+1}^M \frac{2gB_0^\dagger}{E_\mu - E_\nu} \right] \left(\prod_{\eta \neq \nu}^M B_\eta^\dagger \right) |0\rangle \\
& = \sum_{\nu=1}^M B_0^\dagger \left[\sum_{\mu \neq \nu} \frac{2g}{E_\mu - E_\nu} \right] \left(\prod_{\eta \neq \nu}^M B_\eta^\dagger \right) |0\rangle. \quad (C.21)
\end{aligned}$$

Collecting all terms, we obtain

$$\begin{aligned}
H_{\mathcal{U}} |\Psi_M\rangle_{\mathcal{U}} &= \mathbb{E}(M) |\Psi_M\rangle_{\mathcal{U}} + \sum_{\nu=1}^M B_0^\dagger \left[1 - \sum_{j \in \mathcal{U}} \frac{g}{2\epsilon_j - E_\nu} \right] \left(\prod_{\eta \neq \nu}^M B_\eta^\dagger \right) |0\rangle \\
& + \sum_{\nu=1}^M B_0^\dagger \left[\sum_{\mu \neq \nu} \frac{2g}{E_\mu - E_\nu} \right] \left(\prod_{\eta \neq \nu}^M B_\eta^\dagger \right) |0\rangle \\
& = \mathbb{E}(M) |\Psi_M\rangle_{\mathcal{U}} + \sum_{\nu=1}^M B_0^\dagger \left[1 - \sum_{j \in \mathcal{U}} \frac{g}{2\epsilon_j - E_\nu} + \sum_{\mu \neq \nu} \frac{2g}{E_\mu - E_\nu} \right] \left(\prod_{\eta \neq \nu}^M B_\eta^\dagger \right) |0\rangle. \quad (C.22)
\end{aligned}$$

D Rank-one irregular state and irregular vertex operator

Let r denote the rank—the largest integer for which the eigenvalue of the Virasoro generator L_{2r} on the irregular state is nonzero. In the rank-one case ($r = 1$), the irregular state $|I_{\alpha,\gamma}\rangle$ satisfies the following conditions [39, 40]:

$$L_0 |I_{\alpha,\gamma}\rangle = (\Delta_\alpha + \gamma\partial_\gamma) |I_{\alpha,\gamma}\rangle, \quad (\text{D.1})$$

$$L_1 |I_{\alpha,\gamma}\rangle = \gamma(Q - \alpha) |I_{\alpha,\gamma}\rangle, \quad (\text{D.2})$$

$$L_2 |I_{\alpha,\gamma}\rangle = -\frac{\gamma^2}{4} |I_{\alpha,\gamma}\rangle, \quad (\text{D.3})$$

where

$$\Delta_\alpha = \alpha(Q - \alpha), \quad Q = b + \frac{1}{b},$$

and γ is an arbitrary complex parameter.

The irregular state $|I_{\alpha,\gamma}\rangle$ meeting (D.1)-(D.3) is generated from the vacuum $|0\rangle$ by the corresponding rank-one irregular chiral vertex operator (CVO) [19],

$$I_{\alpha,\gamma}(w) \equiv :e^{2\alpha\varphi(w)}e^{\gamma\partial\varphi(w)}:, \quad (\text{D.4})$$

according to the operator-state correspondence, i.e.,

$$\lim_{w \rightarrow 0} I_{\alpha,\gamma}(w) |0\rangle = |I_{\alpha,\gamma}\rangle. \quad (\text{D.5})$$

The rank-one CVO (D.4) consists of ordered exponentials, where $\varphi(w)$ is the free field obeying

$$\langle\varphi(z)\varphi(w)\rangle = -\frac{1}{2}\log(z-w). \quad (\text{D.6})$$

In order to validate that the operator $I_{\alpha,\gamma}(w)$ generates the irregular state $|I_{\alpha,\gamma}\rangle$ it is necessary to compute its OPE with the holomorphic component of the energy-momentum tensor,¹⁶

$$T(z) = -:\partial\varphi(w)\partial\varphi(w): + Q\partial^2\varphi(w), \quad (\text{D.7})$$

and calculate the commutation relations of $I_{\alpha,\gamma}(w)$ with L_0 , L_1 and L_2 . Recall that commutators of the Virasoro generators L_n with the vertex operators $V(w)$ are given by the contour integral,

$$[L_n, V(w)] = \oint_{C_w} \frac{dz}{2\pi i} z^{n+1} T(z) V(w), \quad (\text{D.8})$$

where the contour C_w surrounds w . Indeed, from (D.6) and Wick's theorem one can find the leading singular behavior of the aforementioned OPE:

$$T(z) I_{\alpha,\gamma}(w) = \left(\frac{2\alpha}{z-w} \partial\varphi(w) + \frac{\gamma}{(z-w)^2} \partial\varphi(w) + \frac{\alpha(Q-\alpha)}{(z-w)^2} \right)$$

¹⁶The form (D.7) of $T(z)$ corresponds to 2D CFT with the central charge $c = 1 + 6Q^2$.

$$+ \frac{\gamma(Q-\alpha)}{(z-w)^3} - \frac{\gamma^2}{4} \frac{1}{(z-w)^4} \Big) I_{\alpha,\gamma}(w). \quad (\text{D.9})$$

Next, by making use of the OPE (D.9) and shifting the integration variable $z \rightarrow z + w$ in (D.8) one can compute the commutators:

— for $n = 0$

$$\begin{aligned} [L_0, I_{\alpha,\gamma}(w)] &= \oint_{C_0} \frac{dz}{2\pi i} (z+w) \left(\frac{2\alpha}{z} \partial\varphi(w) + \frac{\gamma}{z^2} \partial\varphi(w) + \frac{\Delta_\alpha}{z^2} \right. \\ &\quad \left. + \frac{\gamma(Q-\alpha)}{z^3} - \frac{\gamma^2}{4} \frac{1}{z^4} \right) I_{\alpha,\gamma}(w) \\ &= (2\alpha w \partial\varphi(w) + \gamma \partial_\gamma + \Delta_\alpha) I_{\alpha,\gamma}(w); \end{aligned} \quad (\text{D.10})$$

— for $n = 1$

$$\begin{aligned} [L_1, I_{\alpha,\gamma}(w)] &= \oint_{C_0} \frac{dz}{2\pi i} (z+w)^2 \left(\frac{2\alpha}{z} \partial\varphi(w) + \frac{\gamma}{z^2} \partial\varphi(w) + \frac{\Delta_\alpha}{z^2} \right. \\ &\quad \left. + \frac{\gamma(Q-\alpha)}{z^3} - \frac{\gamma^2}{4} \frac{1}{z^4} \right) I_{\alpha,\gamma}(w) \\ &= (2\alpha w^2 \partial\varphi(w) + 2\gamma w \partial\varphi(w) + 2w \Delta_\alpha + \gamma(Q-\alpha)) I_{\alpha,\gamma}(w); \end{aligned} \quad (\text{D.11})$$

— for $n = 2$

$$\begin{aligned} [L_2, I_{\alpha,\gamma}(w)] &= \oint_{C_0} \frac{dz}{2\pi i} (z+w)^3 \left(\frac{2\alpha}{z} \partial\varphi(w) + \frac{\gamma}{z^2} \partial\varphi(w) + \frac{\Delta_\alpha}{z^2} \right. \\ &\quad \left. + \frac{\gamma(Q-\alpha)}{z^3} - \frac{\gamma^2}{4} \frac{1}{z^4} \right) I_{\alpha,\gamma}(w) \\ &= \left(2\alpha w^3 \partial\varphi(w) + 3\gamma w^2 \partial\varphi(w) + 3w^2 \Delta_\alpha + 3w\gamma(Q-\alpha) - \frac{\gamma^2}{4} \right) I_{\alpha,\gamma}(w). \end{aligned} \quad (\text{D.12})$$

Finally, by taking the limit

$$\lim_{w \rightarrow 0} L_n I_{\alpha,\gamma}(w) |0\rangle = \lim_{w \rightarrow 0} [L_n, I_{\alpha,\gamma}(w)] |0\rangle$$

for $n = 1, 2, 3$ and implementing (D.10)-(D.12) alongside (D.5), the conditions (D.1)-(D.3) are reproduced.

References

- [1] J. Dukelsky, S. Pittel, G. Sierra, *Colloquium: Exactly solvable Richardson–Gaudin models for many-body quantum systems*, Rev. Mod. Phys. 76, (2004) 643–662.
- [2] P.W. Claeys, *Richardson–Gaudin models and broken integrability*, Thesis (2018), arXiv:1809.04447.
- [3] R.W. Richardson, *A restricted class of exact eigenstates of the pairing-force Hamiltonian*, Phys. Lett. 3 (1963) 277–279.

- [4] R.W. Richardson, N. Sherman, *Exact eigenstates of the pairing-force Hamiltonian*, Nucl. Phys. 52 (1964) 221-238.
- [5] M. Gaudin, *Diagonalisation d'une classe d'Hamiltoniens de spin*, J. Phys. 37 (1976) 1087-1098.
- [6] M. Gaudin, *The Bethe Wavefunction*, Cambridge University Press 2014, Cambridge, translated by J.-S. Caux.
- [7] G. Sierra, *Conformal field theory and the exact solution of the BCS Hamiltonian*, Nucl. Phys. B572 (2000) 517-534, hep-th/9911078.
- [8] J. Von Delft, F. Braun, *Superconductivity in ultrasmall grains: Introduction to Richardson's exact solution*, In: Kulik, I.O., Ellialtioglu, R. (eds) *Quantum Mesoscopic Phenomena and Mesoscopic Devices in Microelectronics*. NATO Science Series, vol 559. Springer, Dordrecht, arXiv:cond-mat/9911058v1.
- [9] G. Ortiz, J. Dukelsky, *BCS-to-BEC crossover from the exact BCS solution*, Phys. Rev. A72 (2005) 043611, arXiv:cond-mat/0503664.
- [10] F. Resare, J. Hofmann, *Few-to-many-particle crossover of pair excitations in a superfluid*, Phys. Rev. A110 (2024) 061302.
- [11] W.-B. He, S. Chesi, H.-Q. Lin, X.-W. Guan, *Quantum dynamics of Gaudin magnets*, Commun. Theor. Phys. 74 (2022) 095102, arXiv:2201.01025.
- [12] A. Faribault, O. El Araby, C. Strater, V. Gritsev, *Gaudin models solver based on the Bethe ansatz/ordinary differential equations correspondence*, Phys. Rev. B 83 (2011) 235124, arXiv:1103.0472.
- [13] A.L. Retore, *Introduction to classical and quantum integrability*, J. Phys. A: Math. Theor. (2022) 55 173001, arXiv:2109.14280v2.
- [14] M.C. Cambiaggio, A.M.F. Rivas, M. Saraceno, *Integrability of the pairing Hamiltonian*, Nucl. Phys. A624 (1997) 157, nucl-th/9708031.
- [15] G. Sierra, *Integrability and conformal symmetry in the BCS model*, Proceedings of the NATO Advanced Research Workshop on Statistical Field Theories, Como 18-23 June 2001, arXiv:hep-th/0111114.
- [16] W. H. Press, S. A. Teukolsky, W. T. Vetterling, B. P. Flannery, *Numerical recipes: The art of scientific computing, Third edition*, Cambridge University Press 2017.
- [17] D. Gaiotto, E. Witten, *Knot invariants from four-dimensional gauge theory*, Adv. Theor. Math. Phys. 16 (2012) 935-1086.
- [18] X. Gu, B. Haghishat, *Liouville conformal blocks and Stokes phenomena*, Beijing J. Pure Appl. Math. 1 (2024) 1, 373-404, arXiv:2311.07960.
- [19] B. Haghishat, Y. Liu, N. Reshetikhin, *Flat Connections from Irregular Conformal Blocks*, Commun. Math. Phys. 406 (2025) 6, 138, arXiv:2311.07960.
- [20] S. Gukov, B. Haghishat, Y. Liu, N. Reshetikhin, *Irregular KZ equations and Kac-Moody representations*, arXiv:2412.16929.

- [21] A.A. Belavin, A.M. Polyakov, A.B. Zamolodchikov, *Infinite conformal symmetry in 2D quantum field theories*, Nucl. Phys. B241 (1984) 333.
- [22] O. El Araby, V. Gritsev, A. Faribault, *Bethe Ansatz and Ordinary Differential Equation Correspondence for Degenerate Gaudin Models*, Phys. Rev. B 85, 115130 (2012), arXiv:1201.5542.
- [23] A. Ciechan, K.I. Wysokinski, *Thermodynamics of the Two-Level Richardson Model*, Acta Physica Polonica Series A (2007) 111(4), DOI: 10.12693/APhysPolA.111.467.
- [24] A. Mironov, A. Morozov, Sh. Shakirov, *Conformal blocks as Dotsenko–Fateev Integral Discriminants*, Int. J. Mod. Phys. A25, 16 (2010) 3173-3207.
- [25] M.R. Piątek, R.G. Nazmitdinov, A. Puente, A.R. Pietrykowski, *Classical conformal blocks, Coulomb gas integrals and Richardson–Gaudin models*, JHEP 04 (2022) 098.
- [26] K. Takemura, *On the eigenstates of the elliptic Calogero–Moser model*, Lett. Math. Phys. 53 (2000) 181-194, arXiv:math/0002104.
- [27] L.F. Alday, Y. Tachikawa, *Affine $SL(2)$ conformal blocks from 4d gauge theories*, Lett. Math. Phys. 94 (2010) 87, arXiv:1005.4469.
- [28] M. Piątek, *Classical torus conformal block, $\mathcal{N} = 2^*$ twisted superpotential and the accessory parameter of Lamé equation*, JHEP 03 (2014) 124, arXiv:1309.7672.
- [29] P. Ghosal, G. Remy, X. Sun, Y. Sun, *Probabilistic conformal blocks for Liouville CFT on the torus*, arXiv:2003.03802.
- [30] H. Desiraju, P. Ghosal, A. Prokhorov, *Proof of Zamolodchikov conjecture for semi-classical conformal blocks on the torus*, arXiv:2407.05839.
- [31] S. Barik, L. Bakker, V. Gritsev, J. Minar, E.A. Yuzbashyan, *Higher spin Richardson–Gaudin model with time-dependent coupling: Exact dynamics*, arXiv:2507.10856.
- [32] J.M. Roman, G. Sierra, J. Dukelsky, *Large N limit of the exactly solvable BCS model: analytics versus numerics*, Nucl. Phys. B634 (2002) 483-510, arXiv:cond-mat/0202070.
- [33] P. Di Francesco, P. Ginsparg, J. Zinn-Justin, *2D Gravity and Random Matrices*, Phys. Rept. 254 (1995) 1-133, arXiv:hep-th/9306153
- [34] B. Eynard, T. Kimura, S. Ribault, *Random matrices*, arXiv:1510.04430
- [35] B. Jurco, *Large N and Bethe ansatz*, Mod. Phys. Lett. A19, 1661 (2004).
- [36] M. Manabe, P. Sułkowski, *Quantum curves and conformal field theory*, Phys. Rev. D95, 126003 (2017), arXiv:1512.05785.
- [37] L. Alday, D. Gaiotto, Y. Tachikawa, *Liouville Correlation Functions from Four-dimensional Gauge Theories*, Lett. Math. Phys. 91 (2010) 167-197, hep-th/0906.3219.
- [38] N.A. Nekrasov, S.L. Shatashvili, *Quantization of Integrable Systems and Four Dimensional Gauge Theories*, XVIth International Congress on Mathematical Physics, pp. 265-289 (2010), arXiv:0908.4052.
- [39] D. Gaiotto, *Asymptotically free $N = 2$ theories and irregular conformal blocks*, J. Phys. Conf. Ser. 462, 012014 (2013), <https://doi.org/10.1088/1742-6596/462/1/012014>.

[40] D. Gaiotto, J. Teschner, *Irregular singularities in Liouville theory and Argyres–Douglas type gauge theories. I.*, JHEP 12 (2012) 050.